Inverse bremsstrahlung absorption rate for super-Gaussian electron distribution functions including plasma screening

M. Sherlock, P. Michel, D. J. Strozzi, L. Divol, E. Kur, and G. Zimmerman*
Lawrence Livermore National Laboratory, Livermore, California 94550, USA

(Received 18 July 2023; revised 2 January 2024; accepted 29 March 2024; published 1 May 2024)

We provide analytic expressions for the effective Coulomb logarithm for inverse bremsstrahlung absorption which predict significant corrections to the Langdon effect and overall absorption rate compared to previous estimates. The calculation of the collisional absorption rate of laser energy in a plasma by the inverse bremsstrahlung mechanism usually makes the approximation of a constant Coulomb logarithm. We dispense with this approximation and instead take into account the velocity dependence of the Coulomb logarithm, leading to a more accurate expression for the absorption rate valid in both classical and quantum conditions. In contrast to previous work, the laser intensity enters into the Coulomb logarithm. In most laser-plasma interactions the electron distribution function is super-Gaussian [Langdon, Phys. Rev. Lett. **44**, 575 (1980)], and we find the absorption rate under these conditions is increased by as much as ≈30% compared to previous estimates at low density. In many cases of interest the correction to Langdon's predicted reduction in absorption is large; for example at $Z = 6$ and $T_e = 400$ eV the Langdon prediction for the absorption is in error by a factor of ≈2. However, we also account for the additional effect of plasma screening, which predicts a reduction in absorption by a similar amount (up to ≈30%). These two effects compete to determine the overall absorption, which may be increased or decreased, depending on the conditions. The corrections can be incorporated into radiation-hydrodynamics simulation codes by replacing the familiar Coulomb logarithm with an analytic expression which depends on the super-Gaussian order "M" and the screening length.

DOI: 10.1103/PhysRevE.109.055201

I. INTRODUCTION

At laser intensities in the range $I \lesssim 10^{16}$ W cm^{-2}, absorption of laser energy by a plasma primarily occurs via the collisional inverse bremsstrahlung process. This is caused by the gain in thermal energy of an electron, at the expense of oscillatory energy, when the electron loses directed momentum as a result of electron-ion scattering. The process is most easily understood in terms of the binary scattering picture [1–3] but can also be derived from linearized Vlasov-Poisson theory [4], which additionally accounts for resonant coupling to plasma waves close to critical density, and Vlasov-Fokker-Planck theory by considering the average power delivered to the isotropic component of the electron distribution by an oscillating electric field [5]. By invoking detailed balance, it can be equated to the bremsstrahlung rate of a plasma in local thermodynamic equilibrium, where the majority of the work which takes into account quantum effects has been carried out. In the bremsstrahlung literature the seminal result was given by Sommerfeld [6,7], who solved for the emission rate during a single electron-ion encounter in the dipole approximation using a partial wave expansion of the electron wave function, accounting for both small and large momentum transfers, corresponding to small and large angle scattering in the classical picture. Karzas and Latter [7] obtained thermally averaged Gaunt factors for a Maxwellian electron distribution, using the Sommerfeld cross section. Quantum effects have also been considered from the perspective of laser absorption and are usually calculated in the Born approximation [8]. The absorption of laser energy is a process of fundamental importance in laser-plasma experiments since it determines the location and extent of heating and overall efficiency. The absorption has recently been measured to high accuracy in well-characterized experimental conditions [9]. Throughout this paper we use SI units unless otherwise stated.

A common feature of previous work is the use of a thermal value for the Coulomb logarithm, which is usually defined in a classical plasma in terms of the maximum ($b_{\max}$) and minimum ($b_{\min}$) impact parameters of relevance, as $\ln \Lambda_t = \ln(\sqrt{1 + b_{\max}^2/b_{\min}^2})$, with subscript "t" denoting "thermal." Note that this thermal logarithm has not been rigorously justified; rather, the use of the thermal velocity inside the logarithm is an *ad hoc* assumption of previous work. If the electrons are weakly coupled, as is the case for the majority of laser-plasma applications, then $b_{\max} = v_t/\omega \equiv b_\omega$ where $v_t = \sqrt{T_e/m}$, T_e is the electron temperature in Joules, m is the electron mass, and ω is the angular frequency of the laser. In the binary scattering picture, electrons that have an impact parameter $b \gtrsim b_\omega$ interact with the laser wave adiabatically because their scattering interaction time is longer than the period of oscillation, justifying the neglect of more distant encounters [1,8,10]. This cutoff also arises naturally in the Vlasov-Poisson theory [4] and the classical theory of free-free bremsstrahlung, where the emission becomes negligible for $b \gtrsim b_\omega$ [11]. In the classical regime, the minimum impact parameter corresponds to that for a $\pi/2$ deflection: $b_{\perp t} = Ze^2/4\pi\varepsilon_0 m v_t^2$, where Z is the ion charge state, ε_0 is the permittivity of free space,

*sherlock3@llnl.gov

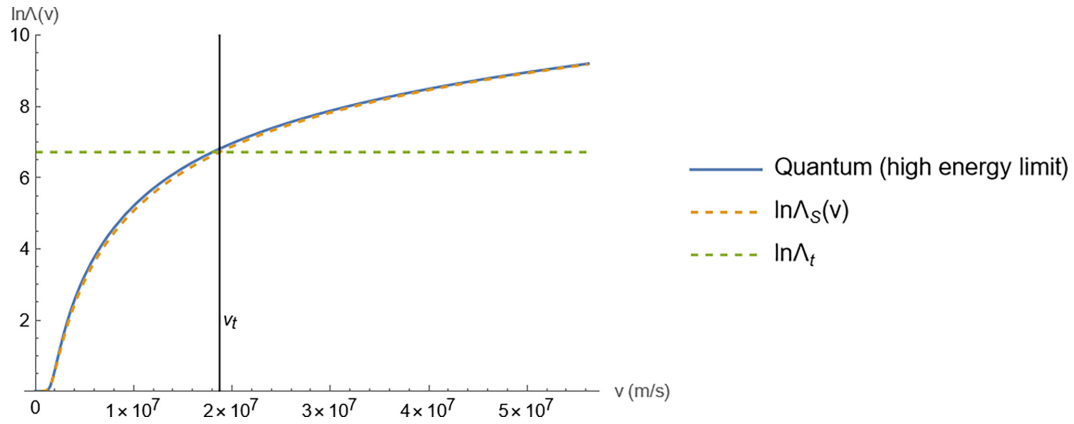

FIG. 1. The velocity-dependent Coulomb logarithm $\ln \Lambda_S(v)$ (orange dashed), the constant "thermal" Coulomb logarithm $\ln \Lambda_t$ (green dashed) and the quantum mechanical result in the limit $\hbar\omega \ll \frac{1}{2}mv^2$ (blue). The vertical line represents the thermal velocity $v_t = \sqrt{T_e/m}$ and the maximum velocity shown corresponds to $3v_t$. The conditions are $Z = 4$, $T_e = 2$ keV and radiation wavelength $\lambda_0 = 0.35$ μm. This calculation neglects plasma screening.

and e is the elementary charge. Under these conditions, the standard thermal, classical, Coulomb logarithm is therefore $\ln \Lambda_t \equiv \ln(\sqrt{1 + b_\omega^2/b_{\perp t}^2})$.

More accurately, we can consider the fact that the Coulomb logarithm depends on the velocity v of each individual electron undergoing scattering, in the form $\ln \Lambda_c(v) = \ln[\sqrt{1 + \{b_{\max}(v)/b_\perp(v)\}^2}]$, where $b_\perp(v) = Ze^2/4\pi\varepsilon_0 mv^2$ and $b_{\max}(v) = v/\omega$, or $\ln \Lambda_c(v) = \ln(\sqrt{1 + \{4\pi\varepsilon_0 mv^3/Ze^2\omega\}^2})$. Although the variation with velocity is weak because it appears under the logarithm, in this paper we show that taking it into account during the average over all electron velocities leads to non-negligible corrections to the absorption rate, especially when the electron distribution function is super-Gaussian. A form for the Coulomb logarithm that we will work with, which provides good accuracy in both the classical and quantum regimes (provided $\hbar\omega \ll \frac{1}{2}mv^2$), is

$$\ln \Lambda_S = \ln \left\{ \sqrt{\frac{b_\omega^2(v) + b_\perp^2(v)}{b_q^2(v) + b_\perp^2(v)}} \right\}, \tag{1}$$

where $b_q(v) = \hbar/2mv$ is the reduced de Broglie wavelength and $b_\omega(v) = v/\omega$. Due to the dependence of $b_\perp$ on Z, approximately speaking, quantum corrections become important for $Z \lesssim 4$ in typical laser-plasma interactions. A plot of $\ln \Lambda_S(v)$ is shown in Fig. 1 for the conditions $Z = 4$ and $T_e = 2$ keV, where it is compared to the thermal logarithm $\ln \Lambda_t$. Clearly we should expect a reduction in absorption at low velocities and an enhancement at high velocities, compared to the thermal logarithm $\ln \Lambda_t$. The form for the logarithm in Eq. (1) is a reasonably accurate fit to the quantum mechanical (Sommerfeld) result in the limit of small $\hbar\omega$, also plotted in Fig. 1. Note that throughout this paper we use the high-energy limit ($\frac{1}{2}mv^2 \gg \hbar\omega$) of the Sommerfeld expression, which we refer to as the quantum high-energy limit. This limit is consistent with the Fokker-Planck approximation and is described in more detail in the Appendix. The fit Eq. (1) becomes erroneous at very low velocities for which the kinetic-energy approaches $\hbar\omega$ and can therefore only be considered accurate enough to estimate the total absorption in plasmas for which $T_e \gg \hbar\omega$. A more accurate, numerical treatment of the absorption which retains finite $\hbar\omega$ contributions in the cross section reveals this region typically contributes only ≈0.5–2.6% to the total absorption due to the lack of electrons in this velocity range. However, a number of other effects contribute to reduce the cross section or introduce uncertainty in this region. Most notably, the inclusion of screening via a Debye potential [12] results in a severely reduced cross section at low velocities which is neglected in the Sommerfeld result and the use of the dipole approximation limits the applicability of the Sommerfeld result to $\frac{1}{2}mv^2 \gtrsim \frac{1}{2}mv_{\rm osc}^2$. Since our focus in this paper is on the study of the effect of super-Gaussian electron distribution functions, we work with the form Eq. (1), because it allows us to capture the most important aspect of the quantum high-energy limit, which is its ability to describe the classical ($b_q \ll b_\perp$), quantum ($b_q \gg b_\perp$), and intermediate ($b_q \approx b_\perp$) regimes. The reduction in absorption at subthermal velocities and the enhancement at high velocities evident in Fig. 1 largely cancel for the case of a Maxwellian electron distribution and the result is close to previous estimates, given in either the classical or Born regimes. However, significant corrections occur for super-Gaussian electron distributions which are a common feature of laser-plasma interactions, and this leads to large corrections to the well-known Langdon effect [5].

In addition to these corrections, the effect of plasma screening must be considered for a wide range of conditions relevant to laser-plasma interactions, and we also provide correction factors that account for this. We have recently reported on the importance of accounting for screening in the interpretation of experimental measurements of the inverse bremsstrahlung absorption rate of a laser passing through well-characterized plasma conditions [9]. Screening reduces the electron-ion radius of interaction which in turn reduces the average scattering rate. Approximately speaking, we expect this effect to become important if the screening length λ_s drops below the maximum impact parameter, i.e., when $\lambda_s \lesssim v/\omega$, so that the appropriate choice of maximum impact parameter becomes $b_{\max} = \min(\lambda_s, v/\omega)$. If electron Debye screening is assumed, $\lambda_s = \lambda_{De} = \sqrt{\varepsilon_o T_e/e^2 n_e}$, then this effect is important for

electrons of velocity $v \gtrsim (\omega/\omega_p)v_t$, where $\omega_p = \sqrt{e^2 n_e/\varepsilon_0 m}$, i.e., the effect becomes increasingly important at high density. The inclusion of ion Debye screening via $\lambda_D = (\lambda_{De}^{-2} + \lambda_{Di}^{-2})^{-1/2}$, where $\lambda_{Di} = \sqrt{\varepsilon_o T_e/Z^2 e^2 n_i}$, typically reduces the screening length further. When the Debye screening is used, the screening length should not be allowed to drop below the ion sphere radius $a_i = (3/4\pi n_i)^{1/3}$, by requiring $\lambda_s = \max(\lambda_D, a_i)$. If instead the ion sphere radius a_i is chosen as the effective screening length to take into account moderate ion coupling, then the condition is even more stringent, affecting a broader range of electrons for which $v \gtrsim a_i\omega$. These issues can be addressed in the calculation of absorption by making use of the cross section for screened Coulomb collisions [13]. Thus, in this paper, we consider two effects: the first, related to the velocity dependence and super-Gaussian distribution, increases the absorption, while the second, accounting for screening, reduces the absorption. Both effects compete to determine the overall absorption, which may be increased or decreased depending on the local plasma conditions. The screening corrections are typically necessary for densities $n_e \gtrsim 0.01 n_c$, where n_c is the critical density.

In Secs. II–V we calculate the effect of the velocity dependence of the Coulomb logarithm on the absorption rate and derive a new effective Coulomb logarithm that accounts for the super-Gaussian form of the electron distribution (but not screening). In Sec. VI we provide the corrections due to screening. The final section (VII), combines and summarizes the results and provides a guide on implementing the corrections in hydrodynamics codes.

II. THEORY

Although we do not account for the Langdon effect self-consistently, we rely on experimental measurements to justify their expected order [14], which are broadly in line with Fokker-Planck simulations that make use of a constant Coulomb logarithm [15]. We have performed Vlasov-Fokker-Planck simulations with a velocity-dependent Coulomb logarithm that confirm this expectation (not shown here). We begin by showing the classical result with a Maxwellian, since the analysis in this case is relatively simple, then we generalize the approach to account for quantum corrections and super-Gaussian distributions. Throughout this paper, we use the common notation 2ω and 3ω to refer to light of wavelength 0.527 and 0.351 μm, respectively. We use the symbols ln and log interchangeably to refer to the natural logarithm.

To motivate the inclusion of velocity dependence in the Coulomb logarithm, we briefly revisit the derivation of the absorption rate in the Vlasov-Fokker-Planck approximation following Langdon [5]. For $v_{\rm osc}/v_t \ll 1$, where the oscillatory velocity $v_{\rm osc}$ is related to the electric field amplitude E_0 via $v_{\rm osc} = eE_0/(m\omega)$, the electron distribution function can be well represented by decomposing it into an isotropic (f_0) and anisotropic (f_1) component with the total distribution given by $f(\boldsymbol{v}) \approx f_0(v) + f_1(v)\cos\theta$, where θ is the angle in velocity space between $\boldsymbol{v}$ and the x axis and the electric field $E_x = E_0 \sin(\omega t)$ is assumed to be directed along x and uniform. An initial phase factor can be included in the oscillation, $\sin(\omega t + \varphi_0)$, but it later drops out and we ignore it here. The assumption that the laser can be represented by such an oscillation also limits us to $v \ll c$ so that there is no appreciable change in the phase of the electron in the motion of the electromagnetic wave during one cycle. Under these conditions, $f_1(v,t)$ evolves according to [5]:

$$\frac{\partial f_1(v,t)}{\partial t} = \frac{eE_0}{m}\sin(\omega t)\frac{\partial f_0(v)}{\partial v} - \nu_{ei}(v) f_1(v,t), \quad (2)$$

where we neglected the time dependence of f_0 because it is assumed to evolve slowly on the timescale of evolution of f_1, and the electron-ion scattering rate $\nu_{ei}(v)$ is defined below. Electron-electron collisional effects on f_1 are neglected because they do not contribute to absorption [1] in the non-relativistic regime. Although this result was obtained in the Fokker-Planck approximation, it is interesting to note that the same expression can be derived from a variety of arguments including the Drude fluid model [3] and the binary scattering model [1], so the result is quite general so long as $v_{\rm osc}/v_t \ll 1$. We also comment that we have successfully obtained the same corrections to absorption as will be presented below by starting instead with the binary scattering model of Pert [1] and dispensing with the $\ln\Lambda = \text{const}$ approximation. However, the mathematics of averaging in time over the laser period is more complicated in this case, but the approach adopted here instead performs the temporal average before the velocity average, which is advantageous in the case of $v_{\rm osc}/v_t \ll 1$. The time-dependent interaction of electrons with induced longitudinal plasma waves has been studied by Dawson [4] who showed this effect is only important close to the critical surface, so this also formally limits our analysis to densities $n_e \ll n_c$, where n_c is the critical density. In practice, these corrections are only significant for $n_e \gtrsim 0.8 n_c$. In our analysis below, we only account for static screening. Except for the very early stages of target ablation during a laser-plasma interaction, the absorption mainly occurs far away from the critical surface in the vast majority of applications of interest. For example, in NIF hohlraum plasmas, most of the absorption occurs at $n_e \lesssim 0.15 n_c$. Since we work in the Fokker-Planck approximation, we are restricted to weakly coupled plasmas, characterized by electron-ion coupling parameter $\Gamma_{Ze} = Ze^2/4\pi\varepsilon_0 a_i T_e \ll 1$, where $a_i = (4\pi n_i/3)^{-1/3}$. However, the weakly coupled regime is of most interest due to the absorption occurring at low density. Approximately speaking, our analysis is only valid for Coulomb logarithms $\ln\Lambda_t \gtrsim 2$ and the extent of the validity of this approximation could be addressed by future molecular dynamics simulations if the computational demands of simulating the weakly coupled regime can be overcome, which is particularly challenging due to the relatively long time taken to establish an equilibrium of the super-Gaussian order. We note that molecular dynamics simulations of other transport processes [16,17] conflict with the long-standing wisdom [18] of restricting the logarithm to $\ln\Lambda_t \geqslant 2$.

The solution to Eq. (2) in the time domain is

$$f_1(v,t) = \frac{eE_0}{m}\frac{\partial f_0(v)}{\partial v} \times \frac{\{\omega e^{-\nu_{ei}(v)t} - \omega\cos(\omega t) + \nu_{ei}(v)\sin(\omega t)\}}{\nu_{ei}(v)^2 + \omega^2}. \quad (3)$$

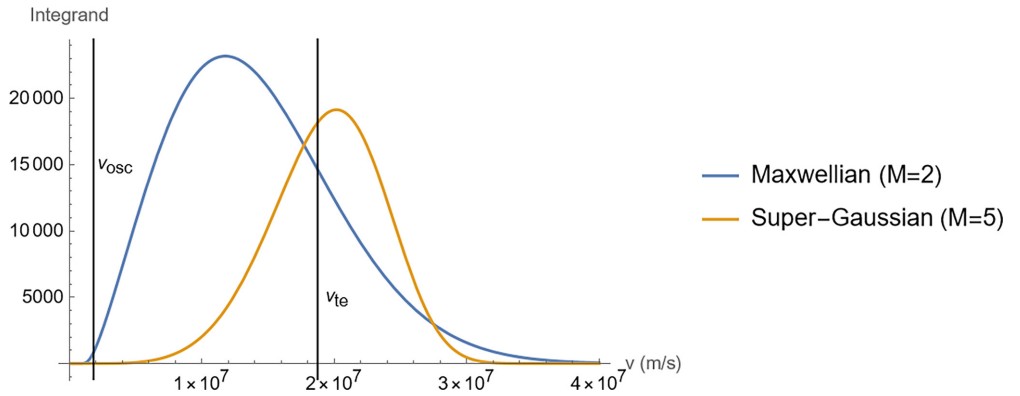

FIG. 2. The integrand which determines the absorption [Eq. (9)], plotted for the case of a Maxwellian ($M = 2$) and a super-Gaussian of order $M = 5$. The locations of the thermal (v_t) and oscillatory (v_{osc}, taken at $I = 1.85 \times 10^{14}$ W cm^{-2} and 2ω) velocities are shown as vertical lines.

For times $\gg \nu_{ei}(v)^{-1}$ and for $\nu_{ei}(v)^2 \ll \omega^2$ this is

$$f_1(v,t) = \frac{eE_0}{m\omega^2}\frac{\partial f_0(v)}{\partial v}\{\nu_{ei}(v)\sin(\omega t) - \omega\cos(\omega t)\}, \quad (4)$$

which corresponds to a small amount of damping superimposed on an oscillation. Note that the condition $\nu_{ei}(v)^2 \ll \omega^2$ imposes a limit on the electron velocity for the validity of Eq. (4) which approximately coincides with the limit imposed by the assumption $\hbar\omega \ll \frac{1}{2}mv^2$. The oscillating electron current density is $j_x = -e\frac{4\pi}{3}\int_0^\infty f_1(v,t)v^3dv$, so the instantaneous power density delivered to the plasma, $\mathbf{j}\cdot\mathbf{E}$, is

$$P = -\frac{e^2E_0^2}{m\omega^2}\frac{4\pi}{3}\int_0^\infty \frac{\partial f_0(v)}{\partial v}\{\nu_{ei}(v)\sin^2(\omega t) - \omega\cos(\omega t)\sin(\omega t)\}v^3dv. \quad (5)$$

Averaging this over one cycle gives:

$$\langle P\rangle = -mv_{osc}^2\frac{2\pi}{3}\int_0^\infty \frac{\partial f_0(v)}{\partial v}\nu_{ei}(v)v^3dv. \quad (6)$$

This is valid so long as f_0 does not vary significantly on the timescale ν_{ei}^{-1}. Although the Fokker-Planck approximation was used, the same result, Eq. (6) can be arrived at from quantum-mechanical arguments [11] for $\hbar\omega \ll T_e$ and $v_{osc}/v_t \ll 1$. We have also performed first-principles classical Monte Carlo simulations of electron-ion scattering, accounting for large-angle collisions from close encounters that confirm the validity of an electron-ion collision operator of the form $-\nu_{ei}(v)f_1(v,t)$ when the plasma is weakly coupled.

For the case of a constant, thermal Coulomb logarithm $\Lambda_t = b_\omega/b_{\perp t}$ with Rutherford scattering, $\nu_{ei}(v) = 4\pi(\frac{Ze^2}{4\pi\varepsilon_0 m})^2\frac{n_i}{v^3}\ln\Lambda_t$ and a Maxwellian electron distribution $f_0 = f_{Max} \equiv \frac{n_e}{4\pi}\sqrt{\frac{2}{\pi}}\frac{1}{v_t^3}\exp(-v^2/2v_t^2)$, the integral in Eq. (6) gives the standard expression for the average absorbed power density:

$$\langle P\rangle_{Max} = \frac{1}{3}\sqrt{\frac{2}{\pi}}\nu_{ei}(v_t)n_e\frac{1}{2}mv_{osc}^2. \quad (7)$$

For the case of a constant Coulomb logarithm and super-Gaussian distribution function of order M, $f_0 = f_{SG} \equiv C_M\frac{n_e}{2^{3/2}v_t^3}\exp(-[\frac{v}{\alpha_e\sqrt{2}v_t}]^M)$, where $C_M = M/(4\pi\alpha_e^3\Gamma[3/M])$ and $\alpha_e^2 = (3/2)\Gamma[3/M]/\Gamma[5/M]$ are defined in terms of the gamma function Γ, the absorption becomes modified by the factor $R \equiv f_{SG}(0)/f_{Max}(0) = \frac{1}{3}\sqrt{\frac{\pi}{6}}M\Gamma(\frac{5}{M})^{3/2}/\Gamma(\frac{3}{M})^{5/2}$ relative to a Maxwellian [5]:

$$\langle P\rangle_{SG} = \frac{A\frac{1}{2}mv_{osc}^2n_e}{9\sqrt{3}v_t^3}\frac{M\Gamma(5/M)^{3/2}}{\Gamma(3/M)^{5/2}}. \quad (8)$$

Approximate parametrizations for the reduction in absorption, $R = \frac{1}{3}\sqrt{\frac{\pi}{6}}M\Gamma(\frac{5}{M})^{3/2}/\Gamma(\frac{3}{M})^{5/2}$, in terms of the laser intensity and plasma conditions, can be found in Ref. [15]. By writing $\nu_{ei}(v) = Av^{-3}\ln\Lambda(v)$ where $A = 4\pi(\frac{Ze^2}{4\pi\varepsilon_0 m})^2n_i$ we see that the more accurate expression for the absorption is in fact:

$$\langle P\rangle = -A\frac{e^2E_0^2}{m\omega^2}\frac{2\pi}{3}\int_0^\infty \frac{\partial f_0(v)}{\partial v}\ln\Lambda(v)dv = Amv_{osc}^2\frac{2\pi}{3}\int_0^\infty f_0(v)\frac{\partial\ln\Lambda(v)}{\partial v}dv. \quad (9)$$

where we assumed $f_0(v)\ln\Lambda(v)|_0^\infty = 0$. In Fig. 2 we have plotted the integrand in Eq. (9) for the case of a Maxwellian f_0 ($M = 2$) and super-Gaussian f_0 of order $M = 5$, along with the location of the thermal (v_t) and oscillatory (v_{osc}, taken at $I = 1.85 \times 10^{14}$ W cm^{-2} and 2ω) velocities. For simplicity, the classical Coulomb logarithm is used here:

$$\ln\Lambda_c(v) = \ln[\sqrt{1 + \{b_{max}(v)/b_\perp(v)\}^2}] = \ln\left[\sqrt{1 + \left(\frac{b_\omega}{b_{\perp t}}\right)^2\left(\frac{v}{v_t}\right)^6}\right]. \quad (10)$$

Figure 2 shows that the absorption increase relative to Langdon is caused by the shift of the integrand to higher velocities as the super-Gaussian order is increased, where the Coulomb logarithm for absorption is greater. Note that the commonly held view that the absorption rate is only dependent on $f_0(v = 0)$ is invalid and this will lead to additional corrections to the absorption arising from nonlocal transport corrections to f_0.

Now we consider plasma conditions for which a classical Coulomb logarithm is valid, $b_{\perp t} \gg \hbar/2mv_t$, and a Maxwellian velocity distribution. Using Eq. (10) in the form

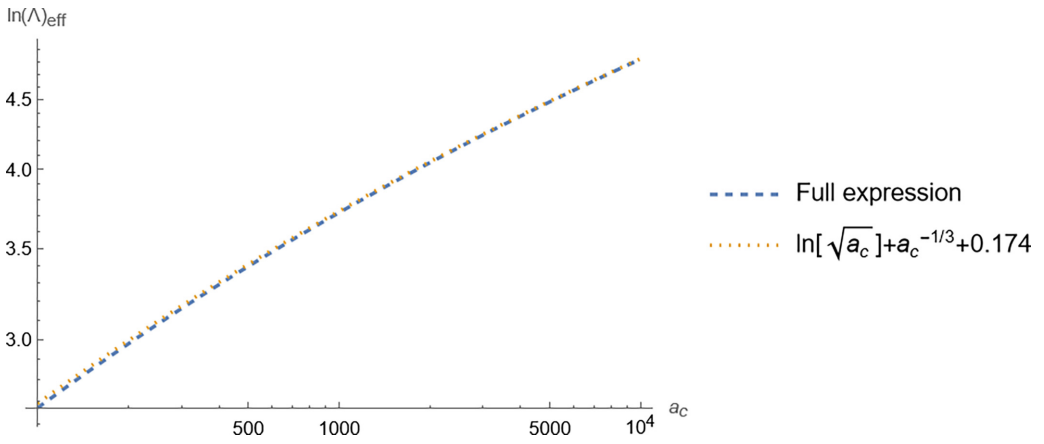

FIG. 3. A comparison of the approximate and full expressions for $\ln \Lambda_{\mathrm{Max},c}(a_c)$, Eqs. (11) and (15).

$\ln \Lambda_c(v) = \ln[\sqrt{1 + a_c(\frac{v}{v_t})^6}]$, where $a_c = (\frac{b_\omega}{b_{\perp t}})^2$, the integral can be done analytically:

$$\langle P\rangle = \frac{9\sqrt{6}Amv_{\mathrm{osc}}^2 n_e a_c G_{1,4}^{4,1}\left(\frac{1}{216a_c}\middle|_{1,\,1,\,\frac{4}{3},\,\frac{5}{3}}^{1}\right)}{\pi^{3/2}v_t^3}, \tag{11}$$

and is expressed in terms of the Meijer G-function, which is simply an integral with known analytic properties enabling us to simplify the result for small argument ($= \frac{1}{216a_c}$ in the above) [19] and rewrite it in terms of more well-known functions. The expression above is valid for all a_c, so long as our expression for $\ln \Lambda_c(v)$ is valid. However, in most regimes of interest the parameter $X \equiv \frac{1}{216a_c}$ is small, so we can Taylor expand the function $G_{1,4}^{4,1}(X)$ in terms of X:

$$\langle P\rangle \approx \frac{P_0 n_e\left\{8\pi^3 X^{1/3} - 3\sqrt{3}\Gamma\left(\frac{1}{3}\right)\Gamma\left(\frac{2}{3}\right)^2\Gamma\left(\frac{4}{3}\right)\ln(X) + 3\sqrt{3}\Gamma\left(\frac{1}{3}\right)\Gamma\left(\frac{2}{3}\right)^2\Gamma\left(\frac{4}{3}\right)\left[\psi^{(0)}\left(\frac{1}{3}\right) + \psi^{(0)}\left(\frac{2}{3}\right) - \gamma\right]\right\}}{24\sqrt{2}\pi^{5/2}\Gamma\left(\frac{2}{3}\right)\Gamma\left(\frac{4}{3}\right)v_t^3}, \tag{12}$$

where γ is the Euler-Gamma constant and $\psi^{(0)}$ is the digamma function and $P_0 = \frac{2\pi}{3}Amv_{\mathrm{osc}}^2$. In obtaining this result, we neglected terms $\propto X^p$ for all $p \geqslant 2/3$. We re-express the term $-3\sqrt{3}\Gamma(\frac{1}{3})\Gamma(\frac{2}{3})^2\Gamma(\frac{4}{3})\ln(X) = 6\sqrt{3}\Gamma(\frac{1}{3})\Gamma(\frac{2}{3})^2\Gamma(\frac{4}{3})\ln(X^{-1/2})$ and replace $X = \frac{1}{216a_c}$:

$$\langle P\rangle \approx \frac{P_0 n_e\left\{8\pi^3 X^{1/3} + 6\sqrt{3}\Gamma\left(\frac{1}{3}\right)\Gamma\left(\frac{2}{3}\right)^2\Gamma\left(\frac{4}{3}\right)\ln(X^{-1/2}) + 3\sqrt{3}\Gamma\left(\frac{1}{3}\right)\Gamma\left(\frac{2}{3}\right)^2\Gamma\left(\frac{4}{3}\right)\left[\psi^{(0)}\left(\frac{1}{3}\right) + \psi^{(0)}\left(\frac{2}{3}\right) - \gamma\right]\right\}}{24\sqrt{2}\pi^{5/2}\Gamma\left(\frac{2}{3}\right)\Gamma\left(\frac{4}{3}\right)v_t^3}. \tag{13}$$

The effective logarithm can be found from $\ln \Lambda_{\mathrm{Max},c} = \frac{\pi^{3/2}2^{3/2}v_t^3}{n_e P_0}\langle P\rangle$,

$$\ln \Lambda_{\mathrm{Max},c} \approx \ln(\sqrt{a_c}) + a_c^{-1/3} + 0.174 \tag{14}$$

or written in terms of the more familiar ratio of impact parameters $\sqrt{a_c} = b_\omega/b_{\perp t}$,

$$\ln \Lambda_{\mathrm{Max},c} \approx \ln\left(b_\omega/b_{\perp t}\right) + \left(b_\omega/b_{\perp t}\right)^{-2/3} + 0.174, \tag{15}$$

where we use subscript "Max,c" to refer to a Maxwellian in the classical approximation. We conclude that the standard thermal Coulomb logarithm $\ln \Lambda_t$ should be replaced by Eq. (15) when the distribution function is Maxwellian, the conditions are classical, and screening can be neglected. This leads to a ≈1–4% increase in the absorption under typical plasma conditions of interest. The approximation 15 is compared to the full expression in Fig. 3.

III. ABSORPTION OF A SUPER-GAUSSIAN DISTRIBUTION FUNCTION VALID FOR CLASSICAL AND QUANTUM CONDITIONS

By building on the above analysis, we now turn to the more involved calculation of the absorption rate, valid in both classical and quantum conditions, for an arbitrary order super-Gaussian electron distribution function. As shown above, Eq. (1) is a good match to the Sommerfeld result across a wide range of velocities (for $\hbar\omega \ll T_e$). We express $\ln \Lambda_S$ in terms of the normalized velocity $w = v/(\alpha_e\sqrt{2}v_t) = v/v_M$, where $v_M = \alpha_e\sqrt{2}v_t$ characterizes the thermal spread of a super-Gaussian, since this simplifies a super-Gaussian function to the form $\propto \exp(-w^M)$:

$$\ln \Lambda_S = \ln\left\{\sqrt{\frac{c_c w^6 + 1}{c_q w^2 + 1}}\right\}, \tag{16}$$

where $c_c = 8a_c\alpha_e^6 = 8(b_\omega^2/b_{\perp t}^2)\alpha_e^6 =$, $c_q = 2(b_{qt}^2/b_{\perp t}^2)\alpha_e^2$, and $b_{qt} = \hbar/2mv_t$ is the thermal reduced de Broglie wavelength, $\alpha_e^2 = (3/2)\Gamma[3/M]/\Gamma[5/M]$, M is the order of the

super-Gaussian and again $b_\omega = v_t/\omega$. The parameter c_q is a measure of the importance of quantum effects, which is $\ll 1$ for classical conditions but $\gtrsim 1$ for quantum conditions, and the parameter c_c can be considered $\gg 1$ for all regimes of interest. Note that in this notation the thermal Coulomb logarithm, $\ln\Lambda_{\rm St}$, is that for $v/v_t = 1$, which corresponds to $w = 1/\sqrt{2}\alpha_e$:

$$\ln\Lambda_{\rm St} = \ln\left\{\sqrt{\frac{\left(b_\omega^2/b_{\perp t}^2\right)+1}{\left(b_{qt}^2/b_{\perp t}^2\right)+1}}\right\}. \tag{17}$$

The absorption is again found from integrating $f_0(w)\partial\ln\Lambda_S(w)/\partial w$, so we require:

$$\frac{\partial\ln\Lambda_S(w)}{\partial w} = \frac{c_q w(2c_c w^6-1)+3c_c w^5}{(c_q w^2+1)(c_c w^6+1)}. \tag{18}$$

This is the key function for correctly accounting for the absorption and further improvements to our work, for example the inclusion of finite $\hbar\omega$ effects, could use this as a starting point. Electrons with a wide range of velocities contribute to absorption, so any approximations valid for small w may be inaccurate. The absorption integral for a Maxwellian is then:

$$\begin{aligned}\langle P\rangle_{M=2} &= P_0\left(C_{M=2}\frac{n_e}{2^{3/2}v_t^3}\right)\int_0^\infty \exp(-w^2)\frac{\partial\ln\Lambda_S(w)}{\partial w}dw \\ &= P_0 C_{M=2}\frac{n_e}{2^{3/2}v_t^3}I_S,\end{aligned} \tag{19}$$

where

$$I_S = \int_0^\infty \exp(-w^2)\frac{\partial\ln\Lambda_S(w)}{\partial w}dw. \tag{20}$$

This integral is challenging to perform analytically for arbitrary M, so we use the *Mathematica* software to provide the result, again in terms of the Meijer G-functions, and rely on a numerical comparison for a verification of the final result, which is

$$I_S = \frac{1}{12\left(c_c-c_q^3\right)}\left\{\frac{\sqrt{3}c_c^{1/3}}{\pi}A_S + B_S\right\} \tag{21}$$

with

$$\begin{aligned}A_S =& 27c_c^{2/3}\left(3c_c-c_q^3\right)G^{4,1}_{1,4}\left(\frac{1}{27c_c}\middle|\begin{matrix}1\\1,\,1,\,\frac{4}{3},\,\frac{5}{3}\end{matrix}\right) \\ &+ c_q\left\{c_q\left[54c_c^{2/3}c_q G^{4,1}_{1,4}\left(\frac{1}{27c_c}\middle|\begin{matrix}0\\0,\,1,\,\frac{4}{3},\,\frac{5}{3}\end{matrix}\right)+G^{4,1}_{1,4}\left(\frac{1}{27c_c}\middle|\begin{matrix}\frac{1}{3}\\0,\,\frac{1}{3},\,\frac{1}{3},\,\frac{2}{3}\end{matrix}\right)+G^{4,1}_{1,4}\left(\frac{1}{27c_c}\middle|\begin{matrix}-\frac{2}{3}\\-\frac{2}{3},\,0,\,\frac{1}{3},\,\frac{2}{3}\end{matrix}\right)\right]\right\} \\ &- c_q\left\{\sqrt[3]{c_c}G^{4,1}_{1,4}\left(\frac{1}{27c_c}\middle|\begin{matrix}\frac{2}{3}\\0,\,\frac{1}{3},\,\frac{2}{3},\,\frac{2}{3}\end{matrix}\right)+\sqrt[3]{c_c}G^{4,1}_{1,4}\left(\frac{1}{27c_c}\middle|\begin{matrix}-\frac{1}{3}\\-\frac{1}{3},\,0,\,\frac{1}{3},\,\frac{2}{3}\end{matrix}\right)\right\},\end{aligned} \tag{22}$$

$$B_S = 6e^{\frac{1}{c_q}}\left(c_c-c_q^3\right)\mathrm{Ei}\left(-\frac{1}{c_q}\right) - 6c_c c_q\left(4c_q^2+c_q-1\right), \tag{23}$$

where Ei is the exponential integral. The quantum corrections are principally accounted for by the term B_S. Relying on $X = \frac{1}{27c_c} \ll 1$, the Meijer G-functions can be Taylor expanded in X, again neglecting terms $\propto X^p$ for all $p \geqslant 2/3$, but retaining terms $\propto X^p \ln X$ for all p. The expansions are given in the Appendix, here we quote the result for $X \ll 1$:

$$\begin{aligned}12\pi I_S \approx& \frac{8\pi^3\sqrt[3]{X}}{\Gamma\left(\frac{2}{3}\right)\Gamma\left(\frac{4}{3}\right)} - 3\sqrt{3}X\Gamma\left(-\frac{2}{3}\right)\Gamma\left(-\frac{1}{3}\right)\ln(X) + 6\pi e^{\frac{1}{c_q}}\mathrm{Ei}\left(-\frac{1}{c_q}\right) - 6\left[4\pi - 9\sqrt{3}\Gamma\left(\frac{4}{3}\right)\Gamma\left(\frac{5}{3}\right)\right]c_q^3 \\ &- 3\left[\sqrt{3}\Gamma\left(\frac{1}{3}\right)\Gamma\left(\frac{2}{3}\right)-2\pi\right]c_q - 3\sqrt{3}\Gamma\left(\frac{1}{3}\right)\Gamma\left(\frac{2}{3}\right)\left[\ln(X)+\gamma-\psi^{(0)}\left(\frac{1}{3}\right)-\psi^{(0)}\left(\frac{2}{3}\right)\right].\end{aligned} \tag{24}$$

Replacing $c_c = \frac{1}{27X}$, and further neglecting terms with numerical prefactors $\ll 1$, for $M = 2$ we find:

$$\begin{aligned}36I_S \approx& \frac{4\pi^2\sqrt[3]{\frac{1}{a_c}}}{\Gamma\left(\frac{2}{3}\right)\Gamma\left(\frac{4}{3}\right)} + \frac{9\sqrt{3}\Gamma\left(\frac{1}{3}\right)\Gamma\left(\frac{2}{3}\right)\left[2\ln(\sqrt{a_c})-\gamma+\ln(216)+\psi^{(0)}\left(\frac{1}{3}\right)+\psi^{(0)}\left(\frac{2}{3}\right)\right]}{\pi} \\ &+ 18e^{\frac{1}{c_q}}\mathrm{Ei}\left(-\frac{1}{c_q}\right) + \frac{9\left[18\sqrt{3}\Gamma\left(\frac{4}{3}\right)\Gamma\left(\frac{5}{3}\right)-8\pi\right]c_q^3}{\pi} + \frac{9\left[3\sqrt{3}\Gamma\left(\frac{2}{3}\right)\Gamma\left(\frac{4}{3}\right)-2\pi\right]c_q^2}{\pi},\end{aligned} \tag{25}$$

where again Ei is the exponential integral. Since I_S represents the effective Coulomb logarithm,

$$\ln\Lambda_{\rm SG}^{M=2} = \ln\left(\sqrt{a_c}\alpha_e^3\right) + 0.9069\sqrt[3]{\frac{1}{a_c\alpha_e^6}} + \frac{1}{2}\exp\left(\frac{1}{c_q}\right)\mathrm{Ei}\left(-\frac{1}{c_q}\right) + 0.1739 \tag{26}$$

or

$$\ln\Lambda_{\rm SG}^{M=2} = \ln\left(\sqrt{a_c}\alpha_e^3\right) + 0.9069a_c^{-1/3}\alpha_e^{-2} + \frac{1}{2}\exp\left(\frac{1}{c_q}\right)\mathrm{Ei}\left(-\frac{1}{c_q}\right) + 0.1739, \tag{27}$$

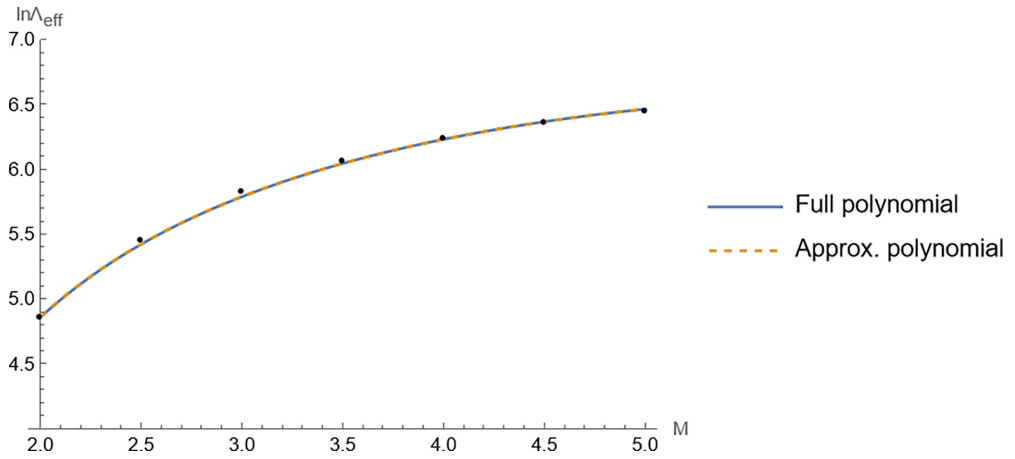

FIG. 4. The polynomial fit for $\ln \Lambda_{\rm SG}$ for various M (blue curve) using Eqs. (27)–(29), for the conditions $Z = 6$ and $T_e = 550$ eV. Numerical evaluations of the integral I_S in Eq. (20) are shown as black dots. The orange dashed curve is an approximation to the full polynomial given by Eqs. (37)–(39).

where the subscript "SG" refers to a super-Gaussian. Although α_e is unity for $M = 2$, we retain it as a parameter in this expression because the appearance of the variable $\sqrt{a_c}\alpha_e^3$ is a common theme across solutions for all M. A comparison of expression 27 to a numerical integration confirms the error is $< 0.1\%$ for $0 < c_q < 100$. Note that the correction we arrived at is a correction to the effective Coulomb logarithm, and it applies *in addition* [20] to the well-known modification to the absorption, R (which appears outside the effective Coulomb logarithm).

We have performed the same analysis for the case $M = 4$ and arrive at

$$\ln \Lambda_{\rm SG}^{M=4} = \ln\left(\sqrt{a_c}\alpha_e^3\right) - 0.785398 e^{-\frac{1}{c_q^2}} \mathrm{erfi}\left(\frac{1}{c_q}\right) + \frac{1}{4} e^{-\frac{1}{c_q^2}} \mathrm{Ei}\left(\frac{1}{c_q^2}\right) + 0.606809, \tag{28}$$

where erfi is the imaginary error function. Again we have left α_e unevaluated. For $M = 6$,

$$\ln \Lambda_{\rm SG}^{M=6} = \ln\left(\sqrt{a_c}\alpha_e^3\right) + \frac{1}{6} e^{\frac{1}{c_q^3}} \mathrm{Ei}\left(-\frac{1}{c_q^3}\right) + 0.225686 c_q^2 - 0.44649 c_q - 0.150458 e^{\frac{1}{c_q^3}} \Gamma\left(-\frac{2}{3}, \frac{1}{c_q^3}\right) + 0.14883 e^{\frac{1}{c_q^3}} \Gamma\left(-\frac{1}{3}, \frac{1}{c_q^3}\right) + 0.751113. \tag{29}$$

In contrast to previous work, the laser intensity now enters the logarithm $\ln(\sqrt{a_c}\alpha_e^3)$ via its influence on α_e. Specifically, since $\alpha_e^2 = (3/2)\Gamma[3/M]/\Gamma[5/M]$ and M can be found from fits in the literature [15] as a function of $\alpha = Z v_{\rm osc}^2/v_t^2$, with $v_{\rm osc}$ obtained from the intensity via $v_{\rm osc} = \frac{e}{m\omega_0}\sqrt{\frac{2I}{c\varepsilon_0}}$. Note that the integrals are significantly more tractable for even M and this is the reason we have excluded odd M from our analysis. However, the value of the effective Coulomb logarithm for arbitrary M can be found from interpolation, because the variation with M is relatively weak. For example, a quadratic spline fit of the form

$$\ln \Lambda_{\rm SG} = aM^2 + bM + c \tag{30}$$

can be used, where $a = (\ln \Lambda_{\rm SG}^{M=2} - 2\ln \Lambda_{\rm SG}^{M=4} + \ln \Lambda_{\rm SG}^{M=6})/8$, $b = (-5\ln \Lambda_{\rm SG}^{M=2} + 8\ln \Lambda_{\rm SG}^{M=4} - 3\ln \Lambda_{\rm SG}^{M=6})/4$, and $c = 3\ln \Lambda_{\rm SG}^{M=2} - 3\ln \Lambda_{\rm SG}^{M=4} + \ln \Lambda_{\rm SG}^{M=6}$. An example of this polynomial fit for $Z = 6$ and $T_e = 550$ eV is shown in Fig. 4 (labeled as "full polynomial") and compared to a numerical evaluation of the integral I_S, showing good agreement. Note that, in the next section we provide more convenient approximations to the analytic expressions presented here, so Eq. (30) is not intended to be used in practical applications.

In Fig. 5 we compare Eq. (30) to the thermal result $\ln \Lambda_t \equiv \ln(\sqrt{1 + b_\omega^2/b_{\perp t}^2})$, plotted as a function of temperature for $Z = 1$ and in Fig. 6 for $Z = 50$. For a Maxwellian, the absorption is enhanced by ≈1–4%, and for a super-Gaussian of order $M = 5$ the absorption is enhanced by ≈30%, demonstrating the importance of accounting for the velocity dependence. The enhancement is approximately uniform across a wide range of temperatures and Z, consistent with the expected scaling predominantly with M, via the dependence of α_e on M.

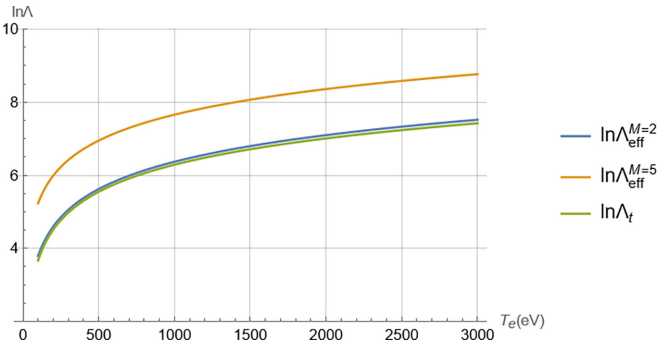

FIG. 5. The polynomial fit for $\ln \Lambda_{\rm SG}(T_e)$ for various $M = 2$ (blue curve) and $M = 5$ (orange curve) for $Z = 1$. For comparison the standard thermal Coulomb log $\ln \Lambda_t$ is also shown (green curve).

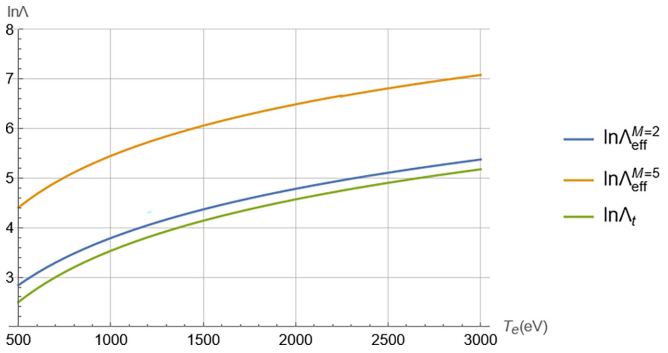

FIG. 6. The polynomial fit for $\ln\Lambda_{\rm SG}(T_e)$ for various $M=2$ (blue curve) and $M=5$ (orange curve) for $Z=50$. For comparison the standard thermal Coulomb log $\ln\Lambda_t$ is also shown (green curve).

It is important to note that although our results predict an increase in absorption compared to the standard Langdon theory [5,15], the overall absorption of a super-Gaussian of order $M>2$ is still less than that for a Maxwellian ($M=2$). The overall reduction in absorption predicted here is given by $R_v = R\ln\Lambda_{\rm SG}/\ln\Lambda_{\rm St}$, where $R \equiv f_{\rm SG}(0)/f_{\rm Max}(0) = \frac{1}{3}\sqrt{\frac{\pi}{6}}M\Gamma(\frac{5}{M})^{3/2}/\Gamma(\frac{3}{M})^{5/2}$ is the standard expectation from previous work, $\ln\Lambda_{\rm SG}/\ln\Lambda_{\rm St}$ accounts for our corrections to the effective Coulomb logarithm, and the subscript "v" refers to velocity dependence. This factor is shown in Fig. 7, where it is clear the reduction in absorption is not as severe as that predicted by Langdon ($=R$). In many cases of interest the correction is large, for example at $Z=6$ and $T_e=400$ eV the Langdon prediction for the absorption is incorrect by a factor >50%. Our results can be viewed as an effective correction to the Langdon effect [5].

IV. ANSATZ SOLUTION

Although our results for $\ln\Lambda_{\rm SG}^{M}$ are analytic, they involve special functions that are not in common use in plasma physics. Here we provide simplified fits that can be evaluated easily, motivated by an intuitive ansatz for $\ln\Lambda_{\rm SG}^{M}$.

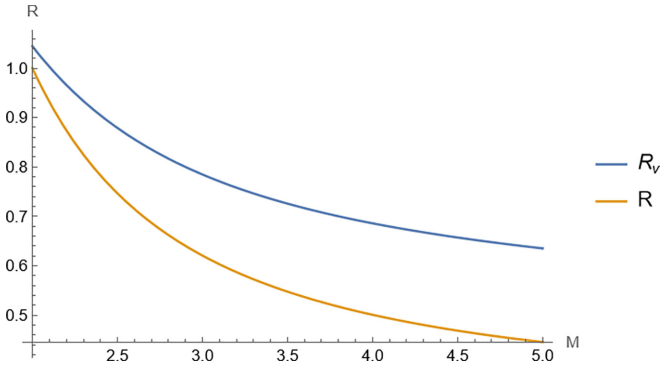

FIG. 7. The overall factor that modifies absorption, R_v, for various super-Gaussian order M (blue curve), compared to the standard Langdon modification R (orange curve), for the conditions $Z=6$ and $T_e=400$ eV.

For $M=2$, we showed above that

$$\ln\Lambda_{\rm SG}^{M=2} = \ln\left(\sqrt{a_c}\alpha_e^3\right) + 0.9069a_c^{-1/3}\alpha_e^{-2} + \frac{1}{2}\exp\left(\frac{1}{c_q}\right){\rm Ei}\left(-\frac{1}{c_q}\right) + 0.1739. \tag{31}$$

The quantum corrections enter in the term $\frac{1}{2}\exp(c_q^{-1}){\rm Ei}(c_q^{-1}) \equiv Q^{M=2}(c_q)$. Returning to our original expression for the velocity-dependent Coulomb logarithm $\ln\Lambda_S(w)$, Eq. (16), if the dominant contribution to the distribution function is near the thermal velocity $w\approx 1$, then we might expect an average Coulomb logarithm of the form

$$\ln\Lambda \approx \ln\left\{\sqrt{\frac{c_c+1}{c_q+1}}\right\} \approx \ln\left\{\sqrt{\frac{8a_c\alpha_e^6+1}{c_q+1}}\right\}, \tag{32}$$

where the form on the right-hand side of Eq. (32) has been motivated by the requirement $\ln\Lambda>0$. This is further supported by noting that the dominant term in $Q^{M=2}(c_q)$ is $\propto \ln(1/\sqrt{c_q})$ when $c_q \gg 1$. In terms of impact parameters, Eq. (32) is

$$\ln\Lambda \approx \ln\left\{\sqrt{\frac{8(b_{\rm max}/b_\perp)^2\alpha_e^6+1}{2\left(b_q/b_\perp\right)^2\alpha_e^2+1}}\right\}. \tag{33}$$

Since we require $b_{\rm max}>b_q$, a more well-behaved form for the above is to replace $b_{\rm max}^2 \to b_{\rm max}^2+b_q^2$:

$$\ln\Lambda \approx \ln\left(\sqrt{\frac{8\alpha_e^6a_c+4\alpha_e^4c_q+1}{c_q+1}}\right). \tag{34}$$

Motivated by these hints, we seek a fit to $\ln\Lambda_{\rm SG}^{M=2}$ of the form

$$\ln\Lambda_{\rm fit}^{M=2} = \ln\left(\sqrt{\frac{8\alpha_e^6a_c+4\alpha_e^4c_q+1}{c_q+1}}\right) + 0.9069\left(\frac{1+c_c}{8}\right)^{-1/3} + r(c_q), \tag{35}$$

where the remainder function $r(c_q)\approx \ln\Lambda_{\rm fit}^{M=2} - \ln\Lambda_{\rm SG}^{M=2}$ should vary weakly with c_q. We have replaced $0.9069a_c^{-1/3}\alpha_e^{-2}$ in Eq. (31) with $0.9069(\frac{1+c_c}{8})^{-1/3}$ to allow sensible behavior at low temperature. We use the following trial form for $r(c_q)$:

$$r(c_q) = \frac{r_0+r_1c_q}{s_0+s_1c_q} \tag{36}$$

and solve for the parameters r_0, r_1, s_0, s_1 by numerical least-squares minimization across the range $10^{-1}\leqslant c_q\leqslant 10^4$, resulting in $r_0=3.074868$, $r_1=0.4457853$, $s_0=3.537712$, and $s_1=0.766085$. The final approximate form for $\ln\Lambda_{\rm SG}^{M=2}$ is then:

$$\ln\Lambda_{\rm fit}^{M=2} = \ln\left(\sqrt{\frac{8\alpha_e^6a_c+4\alpha_e^4c_q+1}{c_q+1}}\right) + 0.9069\left(\frac{1+c_c}{8}\right)^{-1/3} - \frac{r_0+r_1c_q}{s_0+s_1c_q}\left(\frac{c_c}{1+c_c}\right). \tag{37}$$

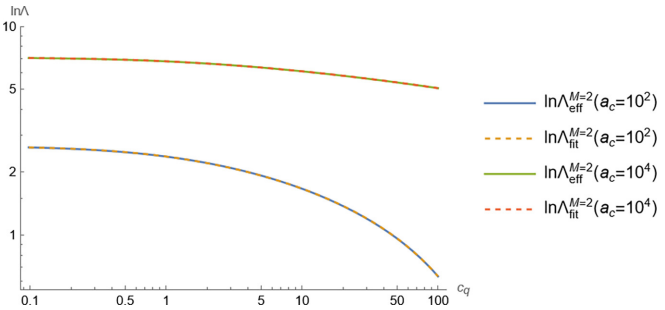

FIG. 8. A comparison of the full expression for $\ln\Lambda_{\rm SG}^{M=2}$ and the approximate fit $\ln\Lambda_{\rm fit}^{M=2}$ as a function of the quantum parameter c_q. Blue and orange curves are for $a_c = 10^2$. Green and red curves are for $a_c = 10^4$.

Note that the factor $c_c/(1+c_c)$ is a further purely *ad hoc* modification to allow sensible ($\ln\Lambda_{\rm fit}^{M} > 0$) behavior at low temperatures. This fit is compared to the full expression Eq. (27) in Fig. 8, showing good agreement across a large range of c_q for two representative choices of a_c.

For $M = 4$ we find similarly:

$$\ln\Lambda_{\rm fit}^{M=4} = \ln\left(\sqrt{\frac{8\alpha_e^6 a_c + 4\alpha_e^4 c_q + 1}{c_q + 1}}\right) + 0.606809 - \frac{r_0 + r_1 c_q}{s_0 + s_1 c_q}\left(\frac{c_c}{1+c_c}\right), \tag{38}$$

with $r_0 = 13.1288$, $r_1 = 4.90536$, $s_0 = 12.6262$, and $s_1 = 5.47617$, which produces similar accuracy to the $M = 2$ case.

Finally, for $M = 6$ we find:

$$\ln\Lambda_{\rm fit}^{M=6} = \ln\left(\sqrt{\frac{8\alpha_e^6 a_c + 4\alpha_e^4 c_q + 1}{c_q + 1}}\right) + 0.751113 - \frac{r_0 + r_1 c_q}{s_0 + s_1 c_q}\left(\frac{c_c}{1+c_c}\right) \tag{39}$$

with $r_0 = 5.1255$, $r_1 = 2.63343$, $s_0 = 4.93054$, and $s_1 = 2.79085$, again with good accuracy.

The absorption for arbitrary M can be found from:

$$\ln\Lambda_{\rm SG} \approx aM^2 + bM + c, \tag{40}$$

now with $a = (\ln\Lambda_{\rm fit}^{M=2} - 2\ln\Lambda_{\rm fit}^{M=4} + \ln\Lambda_{\rm fit}^{M=6})/8$, $b = (-5\ln\Lambda_{\rm fit}^{M=2} + 8\ln\Lambda_{\rm fit}^{M=4} - 3\ln\Lambda_{\rm fit}^{M=6})/4$, and $c = 3\ln\Lambda_{\rm fit}^{M=2} - 3\ln\Lambda_{\rm fit}^{M=4} + \ln\Lambda_{\rm fit}^{M=6}$. This approximate polynomial is compared to the polynomial constructed from the full expressions of the previous chapter in Fig. 4 (orange dashed curve), showing very good agreement. The super-Gaussian index $M(\alpha)$ itself can be found from fits provided by, e.g., Ref. [15] as a function of $\alpha = Zv_{\rm osc}^2/v_t^2$, with $v_{\rm osc}$ obtained from the intensity via $v_{\rm osc} = \frac{e}{m\omega_0}\sqrt{\frac{2I}{c\varepsilon_0}}$. Specifically, $M(\alpha) = 2 + 3/(1 + 1.66/\alpha^{0.724})$.

V. COMPARISON TO QUANTUM MECHANICAL CALCULATION

As a final check on the overall accuracy of our expressions, we compare our polynomial fit to Eqs. (37)–(39), to a numerical evaluation of the high-energy limit Sommerfeld result [6,7] averaged over super-Gaussian distribution functions. Figure 9 shows the case $Z = 1$ and Fig. 10 shows the case $Z = 8$. The fits reproduce the scaling with T_e and M well, with maximum error ≈1.8% for $Z = 8$, $M = 2$, and $T_e \approx 1500$ eV. The main source of discrepancy is simply due to the approximation we begin with, $\ln\Lambda_S$ in Eq. (1), which deviates slightly from the exact Sommerfeld result (see Fig. 1).

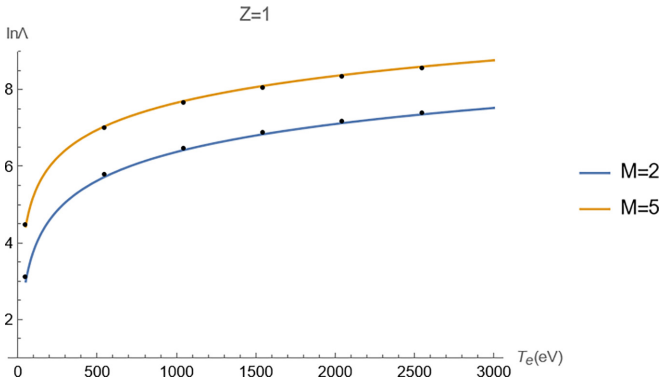

FIG. 9. ($Z = 1$). A comparison of the polynomial constructed from the approximate fits for $\ln\Lambda$, Eqs. (37)–(39), to a numerical integration of the Sommerfeld result. Blue is for $M = 2$, and orange is for $M = 5$. The black dots represent numerical evaluation of the Sommerfeld result.

VI. PLASMA SCREENING CORRECTION

In this section, we present corrections to the absorption rate that arise from plasma screening. If the screening length λ_s in a plasma becomes smaller than the maximum impact parameter $b_\omega(v) = v/\omega$, then the appropriate maximum impact parameter becomes the screening length, because all interactions beyond this distance are curtailed. This scenario has been treated classically [12] and quantum mechanically [13] in the Born approximation, by calculating the velocity-dependent scattering rate in a screened potential. Both theories predict an approximately uniform reduction in the scattering

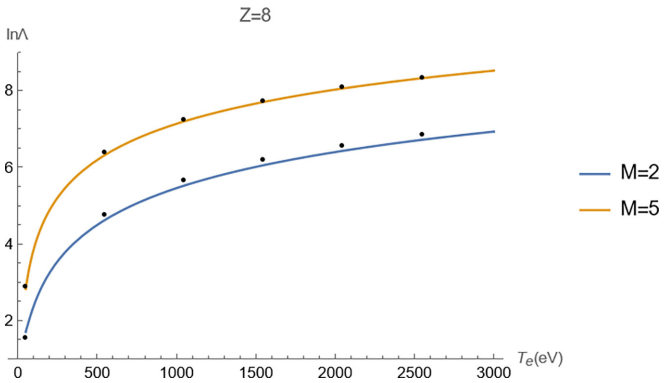

FIG. 10. ($Z = 8$). A comparison of the polynomial constructed from the approximate fits for $\ln\Lambda$, Eqs. (37)–(39), to a numerical integration of the Sommerfeld result. Blue is for $M = 2$, and orange is for $M = 5$. The black dots represent numerical evaluation of the Sommerfeld result.

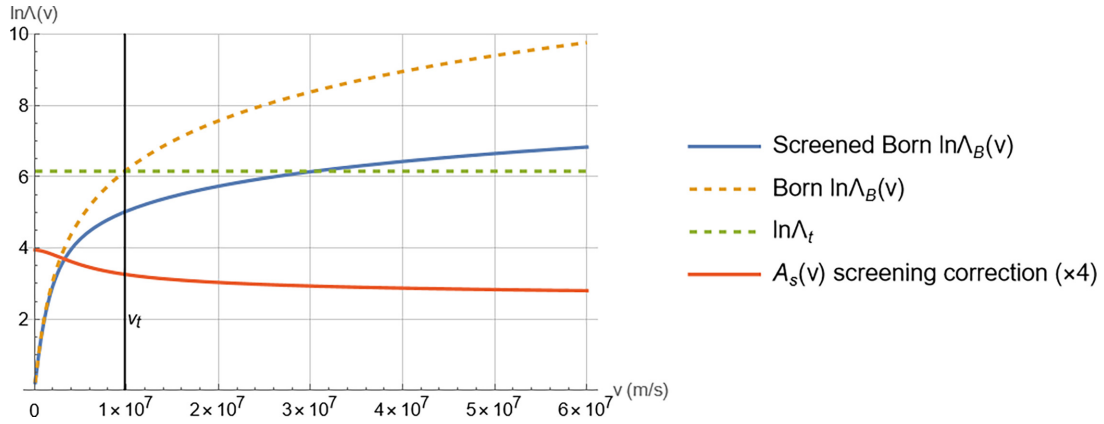

FIG. 11. The Born logarithm and the screened Born logarithm due to Rozsnyai [13]. Also shown is the ratio of the screened-to-unscreened Born result ("screening correction"), and the thermal value for the Coulomb logarithm (in the Born approximation).The screening correction is multiplied by a factor of 4 to make it more visible. The vertical line marks the location of the thermal velocity $v_t = \sqrt{T_e/m}$. The conditions are: $Z = 4$, $n_i = 7.5 \times 10^{25}$, $T_e = 550$ eV, 2ω. The screening length is taken to be $\lambda_s = a_i$.

rate across a wide range of velocities. An example Born result [13] is shown in Fig. 11 for the conditions $Z = 4$, $n_i = 7.5 \times 10^{25}$, $T_e = 550$ eV, 2ω, where we plot both the unscreened and screened Coulomb logarithms for the choice $\lambda_s = a_i$. Also shown is the degree by which the logarithm is reduced due to screening, i.e., the screened-to-unscreened ratio, which we denote $A_s(v)$. This uniformity greatly simplifies the inclusion of screening effects in our calculations, because it can be taken at some characteristic velocity $v = v_{\max}$ (see below) and applied as a separate correction factor, $A_s(v_{\max})$, to obtain the total absorption:

$$\langle P \rangle = A_s(v_{\max}) R \frac{1}{3}\sqrt{\frac{2}{\pi}} \nu_{ei}(v_t) n_e \frac{1}{2} m v_{\rm osc}^2, \tag{41}$$

where $\nu_{ei}(v_t)$ uses $\ln \Lambda_{\rm SG}$ as recommended above and again R is Langdon's standard absorption correction factor for a super-Gaussian. Both the classical and Born screening corrections predict similar reductions in absorption as the screening length λ_s is reduced below b_ω, but we have found via a comparison to numerical calculations that the approximations used to obtain the classical expressions in Ref. [12] are too erroneous (errors ≈20%) for our purposes. This is particularly true near $\lambda_s \approx b_\omega$. For this reason, we use Rozsnyai's result for a fully ionized plasma as the best estimate for the screening correction. However, the result provided by Rozsnyai is relatively complicated and it can be simplified to the following expression by assuming $\frac{1}{2}mv^2 \gg \hbar\omega$:

$$A_s(v) = \frac{\ln\left(\frac{2mv^2}{\hbar\omega}\frac{y}{\sqrt{1+y^2}}\right) - \frac{1}{2}(1+y^2)^{-1}}{\ln\left(\frac{2mv^2}{\hbar\omega}\right)}, \tag{42}$$

where $y \equiv \lambda_s\omega/v$ characterizes the degree of importance of screening and the formula is valid for $y \gtrsim 0.005$ which covers most regimes of interest to laser-plasmas. This formula Eq. (42) is evaluated at the thermal velocity, $A_s(v_t)$, and is plotted alongside the full result given by Rozsnyai [13] in Fig. 12 for the conditions $T_e = 2000$ eV, 3ω, showing close agreement across a wide range of y. $A_s(v_t)$ is useful for estimating the effect of screening for given plasma conditions.

Although the screening correction has only a relatively weak dependence on velocity (see the red curve in Fig. 11), neglecting this dependence when calculating the absorption

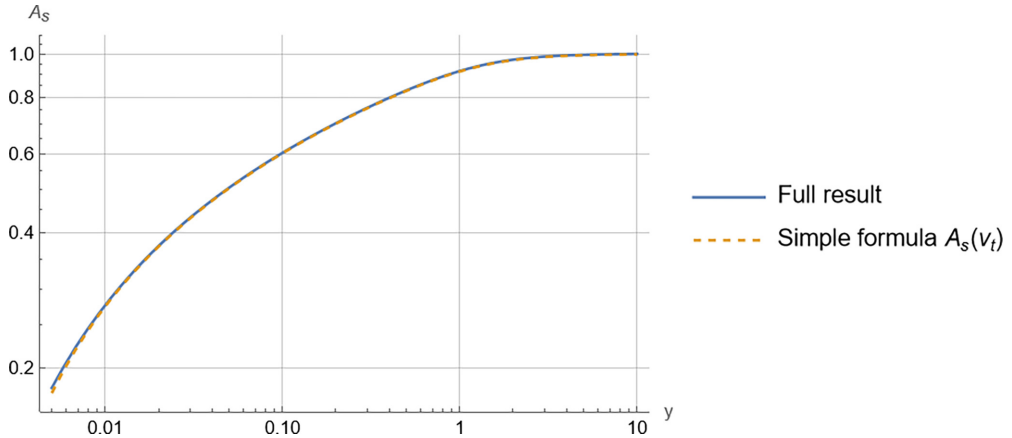

FIG. 12. Modification to the absorption rate, $A_s(v_t)$, calculated in the Born approximation, as a function of $y = \lambda_s/b_\omega = \lambda_s\omega/v_t$. Both the full result [13] and our simple formula Eq. (42) are shown for the conditions $T_e = 2000$ eV, 3ω.

does lead to some error which can be mostly avoided by instead simply evaluating the screening correction at the peak of the function $|\ln\Lambda(v)\partial f_{\rm SG}/\partial v|$, which determines the velocity $v_{\rm max}$ at which the absorption is a maximum [see Eq. (9)]. First, we note that a super-Gaussian of order M has a maximum at the velocity

$$v_r = \frac{(M^2-M)^{1/M}}{M^{2/M}} v_M, \tag{43}$$

where, again, $v_M = \sqrt{2}\alpha_e v_t$. We can find a good approximation to $v_{\rm max}$ by taking advantage of the fact that the logarithmic term is slowly varying with velocity, allowing us to represent the function $|\ln\Lambda(v)\partial f_{\rm SG}/\partial v|$ with a second-order Taylor series, expanding about the point $v = v_r$. The calculation is given in the Appendix for a classical Coulomb logarithm $\ln\sqrt{1+c_c(v/v_M)^6}$, and here we simply state the result, given more succinctly in terms of the normalized velocity $w_r = v_r/v_M$:

$$w_{\rm max} \approx \frac{\Lambda_r^2 w_r \ln\Lambda_r\left[M^2\left(1-3w_r^M+w_r^{2M}\right)+4M\alpha_r+3\right]-12c_c w_r^7\left(2c_c w_r^6+M\alpha_r\Lambda_r-1\right)}{\Lambda_r^2\ln\Lambda_r\left[M^2(1-3w_r^M+w_r^{2M}\right]+3M\alpha_r+2)-6c_c w_r^6(3c_c w_r^6+2M\alpha_r\Lambda_r-3)}, \tag{44}$$

where $\alpha_r = w_r^M - 1$, $\Lambda_r = 1 + c_c w_r^6$, and the velocity of maximum absorption is simply $v_{\rm max} = w_{\rm max} v_M$. To ensure sensible behavior for small Coulomb logarithms, c_c can be replaced with $c_c + c_{\rm min}$, where $c_{\rm min} \approx 50$, in the evaluation of $w_{\rm max}$. The location of $v_{\rm max}$ for super-Gaussian exponents $M = 2$ and $M = 5$ is plotted alongside the function $|\ln\Lambda(v)\partial f_{\rm SG}/\partial v|$ in Fig. 13, for the conditions $T_e = 550$ eV, $n_i = 7.5\times10^{25} m^{-3}$, and $Z = 4$, 2ω, demonstrating the accuracy of the above formula for determining the velocity of peak absorption. The screening correction can then be evaluated at the peak, i.e., $A_s(v_{\rm max})$, and this produces results that are typically within $\epsilon_{\rm err} \lesssim 0.9\%$ of a numerical evaluation of the velocity-dependent integral (see the Appendix).

If Debye screening is considered valid (see Ref. [9] for some comments on this as applied to experiments), then the prescription of Stanton and Murillo [21] can be used for the screening length:

$$\lambda_s = \left(\frac{1}{\lambda_{De}^2} + \frac{1}{\lambda_{Di}^2 + a_i^2}\right)^{-1/2}, \tag{45}$$

where $a_i = (3/4\pi n_i)^{1/3}$ characterizes the interion distance and the $\lambda_{De,i}$ are the usual electron and ion Debye lengths, $\lambda_{De} = (\varepsilon_0 T_e/e^2 n_e)^{1/2}$ and $\lambda_{Di} = (\varepsilon_0 T_i/Z^2 e^2 n_i)^{1/2}$. This form guarantees $\lambda_s \geqslant a_i$, accounting for finite ion coupling strength. As evident in Fig. 12, the effect of screening is to reduce the radius of interaction of electron-ion encounters, which reduces the collisionality. Thus, this effect works in the opposite sense to the corrections we have derived for the super-Gaussian distributions, but in practical applications we find that there are regions in the plasma where one or the other correction dominates.

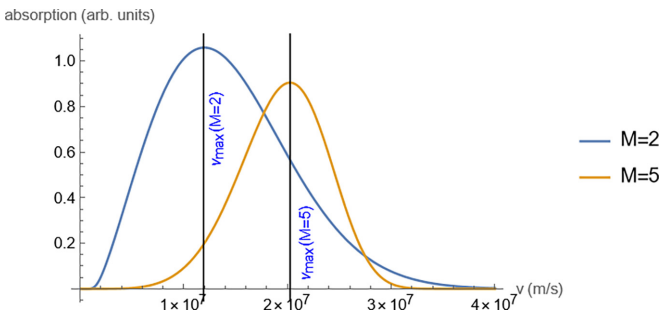

FIG. 13. The integrand which determines the absorption $|\ln\Lambda(v)\partial f_{\rm SG}/\partial v|$, calculated using a classical Coulomb logarithm, plotted for the case of a Maxwellian ($M = 2$), and a super-Gaussian of order $M = 5$. The vertical lines correspond to our expression for the location of the maximum absorption, $v_{\rm max}$, also shown for the cases $M = 2$ and $M = 5$. The conditions are $T_e = 550$ eV, $n_i = 7.5\times10^{25}$ m^{-3}, and $Z = 4$, 2ω.

It is worth pointing out that $\ln\Lambda_{\rm SG}$ represents the Coulomb logarithm which takes into account both velocity dependence and the super-Gaussian distribution function. The screening correction factor A_s is technically also a correction to the Coulomb logarithm itself, so that the overall effective Coulomb logarithm is in fact $\ln\Lambda_{\rm eff} = A_s\ln\Lambda_{\rm SG}$. The integrand [see Eq. (9)] that determines the absorption, $\partial f_0(v)/\partial v\ln\Lambda(v)$, is again plotted in Fig. 14 for the cases $M = 2, 3.5, 5$. In Fig. 14, the solid curves correspond to the unscreened calculation (using $\ln\Lambda_{\rm SG}$), while the dashed curves correspond to the screened calculation (using $\ln\Lambda_{\rm eff} = A_s\ln\Lambda_{\rm SG}$). It is clear that the effect of screening is to simply reduce the absorption almost uniformly across velocity space. In Fig. 15 we show the Maxwellian ($M = 2$) screening correction factor $A_s(v_{\rm max})$ as a function of electron temperature, for the density cases $n_e = 0.01 n_c$ and $n_e = 0.25 n_c$, each calculated for both $Z = 4$ and $Z = 50$ (the wavelength corresponds to 3ω and $\lambda_s = a_i$ was used). The reduction in absorption for these conditions can be as large as ≈30%, and we have found in Ref. [9] that screening corrections are essential to obtain good agreement with experiments.

It should be stressed that the choice $\lambda_s = a_i$, as opposed to $\lambda_s = \lambda_D$, is not rigorously justified, so that these figures are only illustrative. In the experiments of Ref. [9], it was hypothesized that the moderate ion coupling strength, in the range $0.12 \lesssim \Gamma_{ii} \lesssim 0.25$, may result in $\lambda_s \approx a_i$ being the more appropriate choice than the weakly coupled limit $\lambda_s \approx \lambda_D$, although both screening lengths are comparable. For example, with reference to the location $z = 0$ in Fig. 1(b) of Ref. [9], taking $Z = 6$, $T_e = 540$ eV, $T_i = 110$ eV, $n_e = 8.2\times10^{25}$ m^{-3}, we find $\lambda_D = (\lambda_{De}^{-2} + \lambda_{Di}^{-2})^{-1/2} \approx 3.5$ nm and $a_i \approx 2.6$ nm, which results in only a small (≈2%) difference in calculated absorption. Ion screening corrections, in the regime of moderate ion coupling, has already been found to lead to a reduction in absorption in molecular dynamics

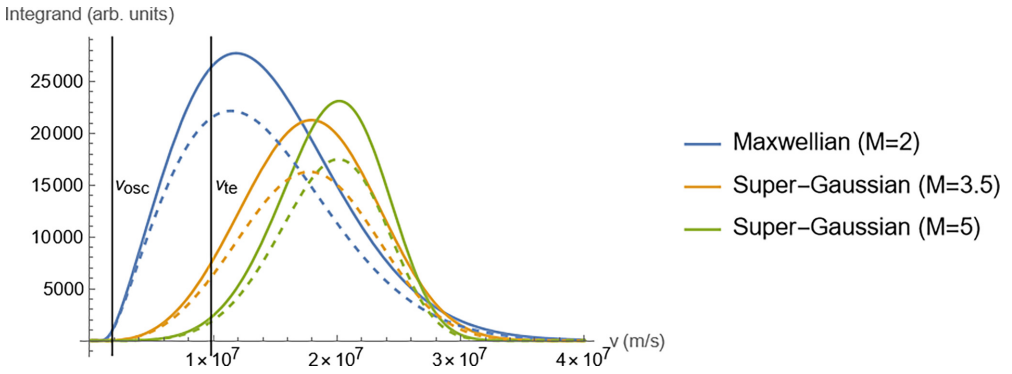

FIG. 14. The integrand which determines the absorption [Eq. (9)] calculated using $\ln \Lambda_s(v)$, plotted for the case of a Maxwellian ($M = 2$), and super-Gaussians of order $M = 3.5$ and $M = 5$. The solid curves show the case without screening, while the dashed curves refer to the case with screening. The ion sphere radius a_i is taken as the screening length. The locations of the thermal (v_t) and oscillatory ($v_{\rm osc}$, taken at $I = 1.85 \times 10^{14}$ W cm^{-2} and 2ω) velocities are shown as vertical lines. The conditions are $T_e = 550$ eV, $n_i = 7.5 \times 10^{25}$ m^{-3}, $Z = 4$, 2ω.

simulations of the inverse bremsstrahlung process [22,23] (for $Z = 1$). A reduction in absorption with increasing density, consistent with a reduced screening length, was also seen in the molecular dynamics simulations of Ref. [24]. These issues should motivate future molecular dynamics simulations to determine the appropriate choice of screening length for moderate ion coupling in the regime $Z > 1$.

VII. PRACTICAL APPLICATION IN HYDRO CODES

We now summarize the steps that need to be taken to calculate the overall absorption rate. Note that the expression for $\ln \Lambda_{\rm SG}$ derived in Sec. III is accurate but relatively complicated. In all practical applications, we therefore use the simpler expression Eq. (40) derived from the ansatz approach of Sec. IV. As stated above [Eq. (41)], the average power density transferred to electron thermal energy is

$$\frac{3}{2} n_e \frac{dT_e}{dt} = A_s(v_{\rm max}) R \frac{1}{3} \sqrt{\frac{2}{\pi}} v_{ei}(v_t) n_e \frac{1}{2} m v_{\rm osc}^2, \tag{46}$$

where $v_{\rm max} = w_{\rm max} v_M$ is the velocity of maximum absorption; $v_M = \sqrt{2}\alpha_e v_t$ characterizes the velocity spread of the super-Gaussian, with $\alpha_e^2 = (3/2)\Gamma[3/M]/\Gamma[5/M]$; and M is the order of the super-Gaussian, which has a maximum at the velocity $v_r = w_r v_M$, where

$$w_r = \frac{(M^2 - M)^{1/M}}{M^{2/M}}. \tag{47}$$

The velocity of maximum absorption is estimated as

$$w_{\rm max} \approx \frac{\Lambda_r^2 w_r \ln \Lambda_r \left[M^2\left(w_r^{2M} - 3w_r^M + 1\right) + 4M\alpha_r + 3\right) - 12 c_c w_r^7 \left(2c_c w_r^6 + M\alpha_r \Lambda_r - 1\right)}{\Lambda_r^2 \ln \Lambda_r \left[M^2\left(w_r^{2M} - 3w_r^M + 1\right) + 3M\alpha_r + 2\right] - 6 c_c w_r^6 \left(3c_c w_r^6 + 2M\alpha_r \Lambda_r - 3\right)}, \tag{48}$$

where $\alpha_r = w_r^M - 1$, $\Lambda_r = 1 + c_c w_r^6$, and $c_c = 8 a_c \alpha_e^6 + c_{\rm min} = 8(b_\omega^2/b_{\perp t}^2)\alpha_e^6 + c_{\rm min}$, with e.g., $c_{\rm min} \approx 50$. Alternatively, if errors of up to ≈5% are regarded as acceptable for the calculation of the screening correction, then the simpler choice of $A_s(v_t)$ can be used in Eq. (46) instead of $A_s(v_{\rm max})$.

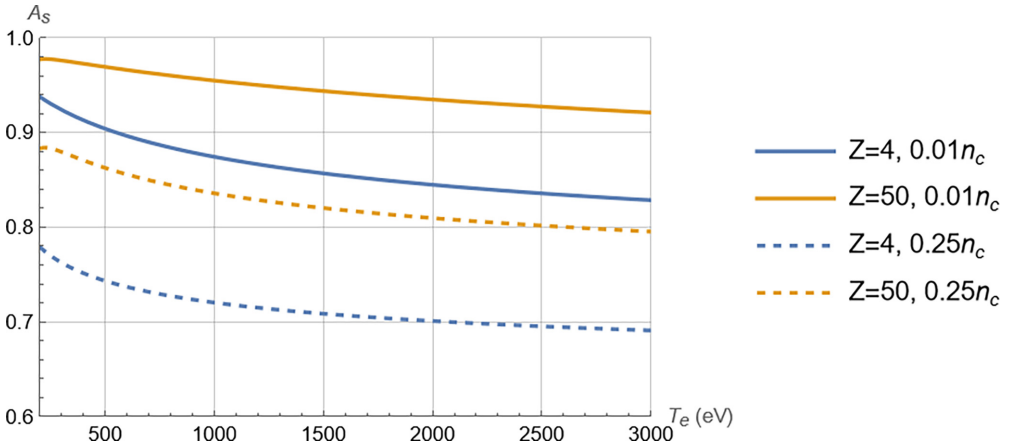

FIG. 15. The screening correction factor $A_s(v_{\rm max})$ for $n_e = 0.01 n_c$ and $n_e = 0.25 n_c$ (at 3ω and $\lambda_s = a_i$). The cases $Z = 4$ and $Z = 50$ are shown for each density, and a Maxwellian is assumed ($M = 2$) for all cases.

In Eq. (46), the electron-ion scattering rate is defined as

$$\nu_{ei}(v) = 4\pi\left(\frac{Ze^2}{4\pi\varepsilon_0 m}\right)^2 \frac{n_i}{v^3}\ln\Lambda_{\rm SG} \tag{49}$$

and the screening correction factor is

$$A_s(v) = \frac{\ln\left(\frac{2mv^2}{\hbar\omega}\frac{y}{\sqrt{1+y^2}}\right) - \frac{1}{2}(1+y^2)^{-1}}{\ln\left(\frac{2mv^2}{\hbar\omega}\right)}, \tag{50}$$

with $y \equiv \lambda_s\omega/v$ and λ_s the screening length. The logarithm $\ln\Lambda_{\rm SG}$ appearing in Eq. (49) is determined from the polynomial fit to the ansatz, Eq. (40), which makes use of the polynomial coefficients (a, b, and c) given under Eq. (40). These coefficients can be found from the three logarithms $\ln\Lambda_{\rm fit}^{M=2}$, $\ln\Lambda_{\rm fit}^{M=4}$, and $\ln\Lambda_{\rm fit}^{M=6}$, which are given by Eqs. (37)–(39). The super-Gaussian order M can be estimated from the fits to Vlasov-Fokker-Planck simulations in Ref. [15] via $M(\alpha) = 2 + 3/(1 + 1.66/\alpha^{0.724})$, where $\alpha = Zv_{\rm osc}^2/v_t^2$, $v_{\rm osc} = \frac{e}{m\omega_0}\sqrt{\frac{2I}{c\varepsilon_0}}$, and $v_t = \sqrt{T_e/m}$. The usual correction to the absorption arising from the Langdon effect, R, is given by $R = \frac{1}{3}\sqrt{\frac{\pi}{6}}M\Gamma(\frac{5}{M})^{3/2}/\Gamma(\frac{3}{M})^{5/2}$, where Γ is the Gamma function.

Again, we note that the overall effective Coulomb logarithm is $\ln\Lambda_{\rm eff} = A_s(v_{\rm max})\ln\Lambda_{\rm SG}$ but the screening correction $A_s(v_{\rm max})$ has been factored out of the collision rate in Eq. (46).

VIII. SUMMARY

We have calculated the absorption rate of laser energy in a weakly coupled plasma, improving on previous work by taking into account the velocity dependence of the Coulomb logarithm, the super-Gaussian nature of the electron distribution function and plasma screening. For the case in which screening can be neglected, our results suggest the absorption is increased over previous estimates by ≈1–4% for a Maxwellian electron distribution and by as much as ≈30% for a super-Gaussian distribution. The reduction in absorption for a super-Gaussian distribution predicted by Langdon is in error by a factor of ≈2, due to the assumption of a constant Coulomb logarithm. However, we have also accounted for the effect of plasma screening, which reduces the electron-ion cross section, leading to a reduction in absorption which can also be as much as ≈30%. Therefore, overall, the absorption rate may be increased or decreased in comparison to previous estimates, depending on the conditions.

The results are valid in both the classical and quantum regimes (provided $\hbar\omega \ll T_e$) and are expressed in terms of an effective Coulomb logarithm for a super-Gaussian distribution function, $\ln\Lambda_{\rm SG}$ [Eq. (40)] and a screening correction factor A_s given by Eq. (50). We provide a polynomial fit to results valid for arbitrary super-Gaussian order M, Eq. (40).

The expressions derived may also have application to free-free emission in plasmas for radiation with $\hbar\omega \ll T_e$.

ACKNOWLEDGMENTS

We gratefully acknowledge useful discussions with D. P. Turnbull, N. Shaffer, C. A. Walsh, W. Rozmus, and M. S. Murillo. We are also grateful to an anonymous referee whose suggestions have significantly improved the quality of this paper. This work was performed under the auspices of the U.S. Department of Energy by LLNL under Contract No. DE-AC52-07NA27344 and release LLNL-JRNL-847776.

APPENDIX A: EXPANSIONS

The Meijer G-functions are a special class of integrals that have useful analytic properties. Here we present the expansions of the Meijer G-functions in terms of $X = \frac{1}{27c_c} \ll 1$ neglecting terms $\propto X^p$ for all $p \geqslant 2/3$. For brevity we only show the expansions for the functions that appear in the case of a Maxwellian ($M = 2$), Eq. (21), although similar analysis has been carried out for $M > 2$,

$$G_{1,4}^{4,1}\left(X\middle|_{1,\,1,\,\frac{4}{3},\,\frac{5}{3}}^{1}\right) \approx X^{2/3}\Gamma\left(-\frac{1}{3}\right)\Gamma\left(-\frac{2}{3}\right)\ln(X) + \Gamma\left(\frac{1}{3}\right)\Gamma\left(\frac{2}{3}\right)X^{-1/3} + \frac{8\pi^3}{3\sqrt{3}\Gamma\left(\frac{2}{3}\right)}\left[\frac{\sqrt[3]{X}}{\Gamma\left(\frac{4}{3}\right)} - \frac{1}{\Gamma\left(\frac{1}{3}\right)}\right], \tag{A1}$$

$$G_{1,4}^{4,1}\left(X\middle|_{0,\,1,\,\frac{4}{3},\,\frac{5}{3}}^{0}\right) \approx X\Gamma\left(\frac{1}{3}\right)\Gamma\left(\frac{2}{3}\right)\ln(X), \tag{A2}$$

$$G_{1,4}^{4,1}\left(X\middle|_{0,\,\frac{1}{3},\,\frac{1}{3},\,\frac{2}{3}}^{\frac{1}{3}}\right) \approx \Gamma\left(\frac{2}{3}\right)\Gamma\left(\frac{4}{3}\right)X^{-2/3} + X^{1/3}\Gamma\left(\frac{1}{3}\right)\Gamma\left(-\frac{1}{3}\right)\ln(X) + \frac{8\pi^3}{3\sqrt{3}\Gamma\left(\frac{1}{3}\right)\Gamma\left(\frac{2}{3}\right)}, \tag{A3}$$

$$G_{1,4}^{4,1}\left(X\middle|_{-\frac{2}{3},\,0,\,\frac{1}{3},\,\frac{2}{3}}^{-\frac{2}{3}}\right) \approx X^{1/3}\left[-\Gamma\left(-\frac{1}{3}\right)\right]\Gamma\left(\frac{1}{3}\right)\ln(X) + X^{1/3}\Gamma\left(\frac{1}{3}\right)\Gamma\left(-\frac{1}{3}\right)\left[\psi^{(0)}\left(\frac{1}{3}\right) + \psi^{(0)}\left(-\frac{1}{3}\right) - \gamma\right] + \frac{8\pi^3}{3\sqrt{3}\Gamma\left(\frac{1}{3}\right)\Gamma\left(\frac{2}{3}\right)} \tag{A4}$$

$$G_{1,4}^{4,1}\left(X\middle|_{0,\,\frac{1}{3},\,\frac{2}{3},\,\frac{2}{3}}^{\frac{2}{3}}\right) \approx X^{2/3}\Gamma\left(-\frac{1}{3}\right)\Gamma\left(-\frac{2}{3}\right)\ln(X) + \Gamma\left(\frac{1}{3}\right)\Gamma\left(\frac{2}{3}\right)X^{-1/3} + \frac{8\pi^3}{3\sqrt{3}\Gamma\left(\frac{2}{3}\right)}\left[\frac{X^{1/3}}{\Gamma\left(\frac{4}{3}\right)} - \frac{1}{\Gamma\left(\frac{1}{3}\right)}\right], \tag{A5}$$

$$G_{1,4}^{4,1}\left(X\middle|_{-\frac{1}{3},\,0,\,\frac{1}{3},\,\frac{2}{3}}^{-\frac{1}{3}}\right) \approx -X^{2/3}\Gamma\left(-\frac{2}{3}\right)\Gamma\left(-\frac{1}{3}\right)\ln(X) - \frac{8\pi^3\left[X^{1/3}\Gamma\left(\frac{1}{3}\right) - \Gamma\left(\frac{4}{3}\right)\right]}{3\sqrt{3}\Gamma\left(\frac{1}{3}\right)\Gamma\left(\frac{2}{3}\right)\Gamma\left(\frac{4}{3}\right)}. \tag{A6}$$

Note that in Eq. (A3), the term in $X^{-2/3}$ appears to be dominant but in the final expression we obtain, it is multiplied by a factor $c_c^{1/3}/(c_c - c_q^3) \approx c_c^{-2/3} \propto X^{2/3}$ rendering it small. This can be seen by considering the prefactors in Eq. (21).

APPENDIX B: QUANTUM GAUNT FACTOR

Sommerfeld [6] obtained the Gaunt factor g_{ff} for photon absorption and emission in the presence of a Coulomb potential by a partial wave analysis, in the dipole approximation. The result, written in terms of the ${}_2F_1$ hypergeometric function has been given by many authors (e.g., Refs. [7,11]):

$$g_{ff} = \frac{2\sqrt{3}}{\pi \eta_i \eta_f}\big[(\eta_i^2 + \eta_f^2 + 2\eta_i^2\eta_f^2)I_0 - 2\eta_i\eta_f\big(1+\eta_i^2\big)^{1/2}\big(1+\eta_f^2\big)^{1/2} I_1\big]I_0, \tag{B1}$$

where

$$I_l = \frac{1}{4}\left[\frac{4k_ik_f}{(k_i-k_f)^2}\right]^{l+1} e^{\pi|\eta_i-\eta_f|/2} \times \frac{|\Gamma(l+1+i\eta_i)\Gamma(l+1+i\eta_f)|}{\Gamma(2l+2)} G_l, \tag{B2}$$

$$G_l = \left|\frac{k_f-k_i}{k_f+k_i}\right|^{i\eta_i+i\eta_f} {}_2F_1 \times \left[l+1-i\eta_f, l+1-i\eta_i; 2l+2; -\frac{4k_ik_f}{(k_i-k_f)^2}\right], \tag{B3}$$

$$\eta_i^2 = \frac{Z^2E_{Ry}}{E_i}, \tag{B4}$$

$$\eta_f^2 = \frac{Z^2E_{Ry}}{E_f}, \tag{B5}$$

with E_{Ry} a Rydberg. In the above, E_i represents the kinetic energy of the electron prior to absorption or emission of a photon of energy $\hbar\omega$, and E_f is the energy afterwards. The energies are related to k_i and k_f via

$$E_i = \frac{\hbar^2k_i^2}{2m}, \tag{B6}$$

$$E_f = \frac{\hbar^2k_f^2}{2m}. \tag{B7}$$

In order to obtain a form for the Gaunt factor compatible with the Fokker-Planck approximation used to obtain the absorption in the presence of nonlinear effects induced by the laser, we require $\hbar\omega \ll E_{i,f}$. This leads us to make the following approximations which we refer to as the quantum high-energy limit:

$$\eta_i^2 + \eta_f^2 + 2\eta_i^2\eta_f^2 \simeq 2\eta_i^2 + 2\eta_i^4, \tag{B8}$$

$$\eta_i\eta_f\big(1+\eta_i^2\big)^{1/2}\big(1+\eta_f^2\big)^{1/2} \simeq \eta_i^2\big(1+\eta_i^2\big), \tag{B9}$$

$$e^{\pi|\eta_i-\eta_f|/2} \simeq 1, \tag{B10}$$

$$\frac{k_f-k_i}{k_f+k_i} \simeq \sqrt{\frac{mE_i}{2\hbar^2}}\frac{\hbar\omega}{E_i(k_f+k_i)}, \tag{B11}$$

$$\frac{k_ik_f}{(k_i-k_f)^2} \simeq 2k_ik_f\frac{\hbar^2}{mE_i}\left(\frac{E_i}{\hbar\omega}\right)^2. \tag{B12}$$

The resulting form for g_{ff} is then valid for electron kinetic energies E much greater than the photon energy, which is typically $\hbar\omega \approx 1$ eV for high power lasers. This limits the validity of our approach to temperatures $\gg 3.5$ eV, which introduces a small error for laboratory conditions associated with the low-energy electrons for which $E \approx \hbar\omega$, despite the lack of electrons at low energy in a Maxwellian electron distribution. For example, the total absorption rate for a Maxwellian plasma, according to the full Sommerfeld expression Eq. (B1) with $Z = 4$, $T_e = 550$ eV is increased over the high-energy limit by ≈2.6%. For the conditions $Z = 50$, $T_e = 3500$ eV, the increase is ≈0.5%. The error arises from the fact that the full Sommerfeld result Eq. (B1) is ≈1 when $E \lesssim \hbar\omega$, whereas our high-energy limit expression is close to zero for this energy range. We can estimate the scaling of the error for the case of a Maxwellian velocity distribution by considering that the neglected contribution to the absorption integral occurs for energies $\frac{1}{2}mv^2 \lesssim \hbar\omega \equiv \frac{1}{2}mv_c^2$, which defines a cutoff velocity v_c below which the error is significant. With reference to Eq. (9), the error scaling is approximately given by

$$\epsilon_{\rm err} \approx \frac{\frac{\pi}{\sqrt{3}}\left|\int_0^{v_c}\frac{\partial f_M(v)}{\partial v}g_{ff}(v)dv\right|}{\left|\int_0^{\infty}\frac{\partial f_M(v)}{\partial v}\ln\Lambda(v)dv\right|}. \tag{B13}$$

To avoid the complications of evaluating the full integrals, we use the simplified velocity dependence for the logarithm:

$$\ln\Lambda(v) = \ln\left\{1+\alpha\left(\frac{v}{v_t}\right)^n\right\}, \tag{B14}$$

where α characterizes the expected thermal value of Λ (i.e., $\ln\Lambda_t \approx \ln\alpha$) and $n = 3$ applies to classical conditions, while $n = 2$ applies to quantum conditions. Taking $g_{ff}(v) \approx 1$ for the integral in the numerator, and assuming $(v_c/v_t)^2 \ll 1$, the error evaluates to

$$\epsilon_{\rm err} \approx \frac{\pi}{\sqrt{3}}\left\{1-\exp\left(-\frac{v_c^2}{2v_t^2}\right)\right\}\frac{1}{\ln\Lambda} \approx \frac{\pi}{\ln\Lambda\sqrt{3}}\frac{\hbar\omega}{T_e}, \tag{B15}$$

so that our quantum high-energy limit is accurate so long as $\hbar\omega \ll T_e$ and $\ln\Lambda$ is not too small (consistent with the above numerical estimates). Note that, technically, we have only estimated the scaling of the error rather than the magnitude, because v_c does not determine the region of error with high accuracy.

However, the Sommerfeld result neglects plasma screening, which is known (classically, at least) to severely reduce the cross section at low energies [12], so that the Sommerfeld result is likely invalid at low energy in a plasma for this reason. Therefore we expect the maximum possible error incurred by working in the high-energy limit to be in accordance with the above estimates but the more likely error to be lower than this. Without a quantum theory of scattering including plasma effects, we are unable to obtain an accurate estimate of the error associated with the assumption $E \gg \hbar\omega$. We note that there are a number of other issues which are unresolved at low electron velocities: The assumption $\nu_{ei}(v) \ll \omega_0$ is only valid for sufficiently high electron velocities; the validity of a Maxwell-Boltzmann velocity distribution at low velocities

is questionable due to the importance of electron coupling at low velocity; finite $\frac{1}{2}mv_{\rm osc}^2$ effects are important at low velocity. These issues associated with the cross section would need to be addressed, along with understanding the validity of the Markov approximation for low-energy electrons if greater accuracy is to be achieved.

APPENDIX C: ESTIMATE OF THE VELOCITY OF PEAK ABSORPTION

Here we provide an estimate of the location of peak absorption in velocity space. As mentioned in the main text, the peak of the function $-\ln\Lambda(v)\partial f_{\rm SG}/\partial v$ determines the velocity $v_{\rm max}$ at which the absorption is a maximum. In general, it is not possible to find an analytic expression for $v_{\rm max}$, but we can find a good approximation to $v_{\rm max}$ by taking advantage of the fact that the logarithmic term is slowly varying with velocity. We work with the normalized velocity $w = v/v_M$ and use a generic classical logarithm for simplicity, so that

$$\ln\Lambda(w) = \tfrac{1}{2}\ln\{1 + c_c w^6\} \tag{C1}$$

and look for solutions to $\partial\{\ln\Lambda(w)\partial f_{\rm SG}/\partial w\}\partial w = 0$. First we determine the velocity of the maximum of the function $\partial f_{\rm SG}/\partial w$, which is

$$w_r = \frac{(M^2 - M)^{1/M}}{M^{2/M}}. \tag{C2}$$

Then we assume that the maximum of the function $\ln\Lambda(w)\partial f_{\rm SG}/\partial w$ is close to w_r, which enables us to represent $\ln\Lambda(w)\partial f_{\rm SG}/\partial w$ as a second-order Taylor series about the point $w = w_r$:

$$\frac{1}{4}Me^{-w_r^M}w_r^{M-3}\{A_0 + A_1(w - w_r) + A_2(w - w_r)^2\}, \tag{C3}$$

$$A_0 = 2w_r^2\ln\Lambda_r, \tag{C4}$$

$$A_1 = -\frac{2w_r\left[\Lambda_r(M\alpha_r + 1)\ln\Lambda_r - 6c_c w_r^6\right]}{\Lambda_r}, \tag{C5}$$

$$A_2 = \ln\Lambda_r\left[M^2\left(-3w_r^M + w_r^{2M} + 1\right) + 3M\alpha_r + 2\right] - \frac{6c_c w_r^6\left(3c_c w_r^6 + 2M\alpha_r\Lambda_r - 3\right)}{\Lambda_r^2}, \tag{C6}$$

where $\alpha_r = w_r^M - 1$ and $\Lambda_r = 1 + c_c w_r^6$. The location of the maximum of $|\ln\Lambda(w)\partial f_{\rm SG}/\partial w|$ can then be approximated as the location of the maximum of the above function, which is

$$w_{\rm max} = \frac{\Lambda_r^2 w_r\ln\Lambda_r\left[M^2\left(w_r^{2M} - 3w_r^M + 1\right) + 4M\alpha_r + 3\right] - 12c_c w_r^7\left(2c_c w_r^6 + M\alpha_r\Lambda_r - 1\right)}{\Lambda_r^2\ln\Lambda_r\left[M^2(w_r^{2M} - 3w_r^M + 1) + 3M\alpha_r + 2\right] - 6c_c w_r^6\left(3c_c w_r^6 + 2M\alpha_r\Lambda_r - 3\right)}, \tag{C7}$$

from which it follows $v_{\rm max} = v_M w_{\rm max}$. The ability of this expression to accurately estimate the location of peak absorption is shown in Fig. 13 in the main text. We plot the above expression for $w_{\rm max}$ as a function of M in Fig. 16 (blue curve labeled $c_q = 0$) for $c_c = 10^5$, which shows that the naive choice $v_{\rm max} \approx v_M$ (corresponding to $w_{\rm max} \approx 1$) is most erroneous at small M. This is because the Coulomb logarithm changes more rapidly with v at lower v, and a Maxwellian has a maximum at lower v than does a super-Gaussian.

When this expression is used to calculate the absorption by replacing the full velocity integration over $A_s(v)$ with the factor $A_s(v_{\rm max})$, the error can be estimated as $\epsilon_{\rm err} = 1 - |A_s(v_{\rm max})\int_0^\infty \partial f_{\rm SG}/\partial v\ln\Lambda(v)dv|/|\int_0^\infty A_s(v)\partial f_{\rm SG}/\partial v\ln\Lambda(v)dv|$, where the integrals are carried out numerically. For the conditions $Z = 50$, $T_e = 3$ keV, 3ω, $n_e = 10^{27}$ m^{-3}, the error is $\epsilon_{\rm err} = 0.004$, $\epsilon_{\rm err} = 0.009$, and $\epsilon_{\rm err} = 0.007$ for $M = 2$, $M = 3.5$, and $M = 5$, respectively. For the conditions $Z = 4$, $T_e = 550$ eV, 3ω, $n_i = 2.5\times10^{26}$ m^{-3}, the error is $\epsilon_{\rm err} = 0.006$, $\epsilon_{\rm err} = 0.008$, and $\epsilon_{\rm err} = 0.008$ for $M = 2$, $M = 3.5$, and $M = 5$, respectively.

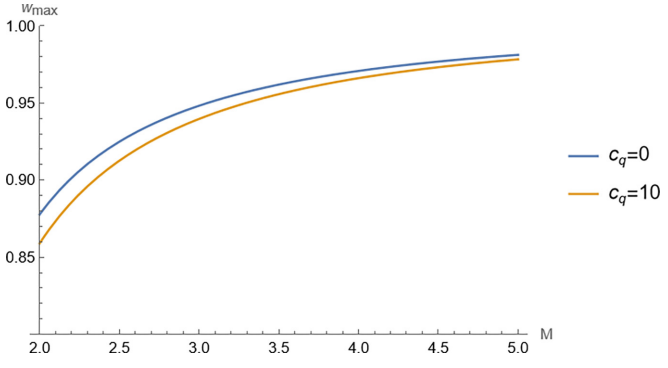

FIG. 16. The normalized velocity of maximum absorption $w_{\rm max}$, plotted as a function of M for the case $c_c = 10^5$. The blue curve shows the case for a purely classical Coulomb logarithm, while the orange curve includes quantum effects with $c_q = 10$.

Although we have assumed a classical form for the Coulomb logarithm, the result Eq. (C7) tends to work well even when quantum effects are important. This can be shown by carrying out the same analysis as above, but with a more general form for the logarithm:

$$\ln\Lambda(w) = \frac{1}{2}\ln\left\{\frac{1 + c_c w^6}{1 + c_q w^2}\right\}, \tag{C8}$$

which yields

$$w_{\rm max} = w_r - \frac{w_r^3}{C_1 + C_2 + C_3} \times\left\{\frac{c_q\left(4c_c w_r^6 - 2\right) + 6c_c w_r^4}{\Lambda_{\rm rc}\Lambda_{\rm rq}} - \frac{(M\alpha_r + 1)\ln\Lambda_r}{w_r^2}\right\}, \tag{C9}$$

where

$$C_1 = \ln\Lambda_r\left\{M^2\left(w_r^{2M} - 3w_r^M + 1\right) + 3M\alpha_r + 2\right\}, \quad \text{(C10)}$$

$$C_2 = \frac{2w_r^2}{\Lambda_{\rm rc}^2\Lambda_{\rm rq}^2}\left\{c_q^2\left(17c_c w_r^8 + w_r^2 - 2c_c^2 w_r^{14}\right) + c_q\left(28c_c w_r^6 - 7c_c^2 w_r^{12} - 1\right) - 3c_c w_r^4\left(c_c w_r^6 - 5\right)\right\}, \quad \text{(C11)}$$

$$C_3 = -\frac{4w_r^2(M\alpha_r + 1)\left[c_q\left(2c_c w_r^6 - 1\right) + 3c_c w_r^4\right]}{\Lambda_{\rm rc}\Lambda_{\rm rq}}, \quad \text{(C12)}$$

$$\Lambda_{\rm rq} = 1 + c_q w_r^2, \quad \text{(C13)}$$

$$\Lambda_{\rm rc} = 1 + c_c w_r^6, \quad \text{(C14)}$$

and note that the definition of Λ_r now corresponds to the general form for the Coulomb logarithm:

$$\Lambda_r = \frac{1 + c_c w_r^6}{1 + c_q w_r^2}. \quad \text{(C15)}$$

This result recovers the classical result [Eq. (C7)] when $c_q \to 0$, and is plotted in Fig. 16 for a case in which quantum corrections are large, $c_q = 10$ (and again, $c_c = 10^5$). Since this result is close to the classical result, in the main text we recommend only the classical result, to keep the model relatively easy to implement, but the model presented above might be useful if increased accuracy is required in the quantum regime. Note that the small error in $w_{\rm max}$ in quantum conditions, evident in Fig. 16, leads to an even smaller error in the actual absorption estimate, meaning the use of a classical Coulomb logarithm for determining $w_{\rm max}$ is largely acceptable.

[1] G. J. Pert, J. Phys. A **5**, 506 (1972).
[2] F. B. Bunkin *et al.*, Sov. Phys. Usp. **15**, 416 (1973).
[3] P. Mulser, F. Cornolti, E. Bésuelle, and R. Schneider, Phys. Rev. E **63**, 016406 (2000).
[4] J. Dawson and C. Oberman, Phys. Fluids **5**, 517 (1962).
[5] A. B. Langdon, Phys. Rev. Lett. **44**, 575 (1980).
[6] A. J. Sommerfeld, *Atombau und Spektralinien* (Vieweg & Sohn, Braunschweig, 1939), Vol. II, Chap. 7, Sec. 5.
[7] W. J. Karzas and R. Latter, Astrophys. J. Suppl. Ser. **6**, 167 (1962).
[8] S. Skupsky, Phys. Rev. A **36**, 5701 (1987).
[9] D. Turnbull, J. Katz, M. Sherlock, L. Divol, N. R. Shaffer, D. J. Strozzi, A. Colaitis, D. H. Edgell, R. K. Follett, K. R. McMillen, P. Michel, A. L. Milder, and D. H. Froula, Phys. Rev. Lett. **130**, 145103 (2023).
[10] D. J. Jackson, *Classical Electrodynamics*, 3rd ed. (Wiley, New York, 1987).
[11] G. Bekefi, *Radiation Processes in Plasmas* (Wiley, New York, 1973).
[12] R. L. Liboff, Phys. Fluids **2**, 40 (1959).
[13] B. F. Rozsnyai, J. Quant. Spectroscop. Radiat. Transf. **22**, 337 (1979).
[14] A. L. Milder, J. Katz, R. Boni, J. P. Palastro, M. Sherlock, W. Rozmus, and D. H. Froula, Phys. Rev. Lett. **127**, 015001 (2021).
[15] J. P. Matte, M. Lamoureux, C. Moller, R. Y. Yin, J. Delettrez, J. Virmont, and T. W. Johnston, Plas. Phys. Control. Fusion **30**, 1665 (1988).
[16] D. O. Gericke, M. S. Murillo, and M. Schlanges, Phys. Rev. E **65**, 036418 (2002).
[17] B. Scheiner and S. D. Baalrud, Phys. Rev. E **100**, 043206 (2019).
[18] Y. T. Lee and R. M. More, Phys. Fluids **27**, 1273 (1984).
[19] I. S. Gradshteyn, *Tables of Integrals, Series, and Products*, 6th ed. (Academic Press, San Diego, CA, 2000).
[20] By "addition" we mean "as well as", not "in summation with."
[21] L. G. Stanton and M. S. Murillo, Phys. Rev. E **93**, 043203 (2016).
[22] P. Hilse, M. Schlanges, T. Bornath, and D. Kremp, Phys. Rev. E **71**, 056408 (2005).
[23] Th. Bornath, D. Kremp, P. Hilse, and M. Schlanges, J. Physics: Conf. Ser. **11**, 180 (2005).
[24] N. David, D. J. Spence, and S. M. Hooker, Phys. Rev. E **70**, 056411 (2004).